SRI International

AD-A274 249

AEOSR-TR· ~~~ 0900

Final Report • November

HIGH-SPEED, HIGH-DENSITY, COHERENT TIME-DOMAIN OPTICAL MEMORY

Prepared by:

Ravinder Kachru, Senior Research Physicist
Xiao-An Shen, Postdoctoral Fellow
Molecular Physics Laboratory

93-31291

DTIC
ELECTE
DEC 3 0 1993
S
A

SF

93 12 27 0

333 Ravenswood Avenue • Menlo Park, CA 94025-3493 • (415) 326-6200 • FAX: (415) 326-5512 • T

REPORT DOCUMENTATION PAGE

Form Approved
OMB No. 0704-0188

1. AGENCY USE ONLY *(Leave blank)*	2. REPORT DATE November 1993	3. REPORT TYPE AND DATES COVERED Final Report 1 Sep 90 - 31 Aug 93

4. TITLE AND SUBTITLE
High-Speed, High-Density, Coherent Time-Domain
Optical Memory

5. FUNDING NUMBERS
C:F-49620-90-C-0083

6. AUTHOR(S)
R. Kachru, and X-A. Shen

7. PERFORMING ORGANIZATION NAME(S) AND ADDRESS(ES)
SRI International
333 Ravenswood Avenue
Menlo Park, CA 94025

8. PERFORMING ORGANIZATION REPORT NUMBER
MP 93-225

9. SPONSORING/MONITORING AGENCY NAME(S) AND ADDRESS(ES)
Air Force Office of Scientific Research
Building 410
Bolling Air Force Base, DC 20332-6448

10. SPONSORING/MONITORING AGENCY REPORT NUMBER
2305/DS

11. SUPPLEMENTARY NOTES

12a. DISTRIBUTION/AVAILABILITY STATEMENT

Approved for public release; distribution unlimited

12b. DISTRIBUTION CODE

13. ABSTRACT *(Maximum 200 words)*

The objective of this research was to quantitatively evaluate the concept of time-domain optical memory (TDOM) using the hole-burning mechanism. The TDOM concept offers both high speed and high memory density. The advantage of TDOM over traditional semiconductor memory is its inherent parallelism, which allows data to be stored and retrieved from the memory at much higher speed. The practical success of the proposed memory, therefore, depends critically on—among other issues—the storage, retrieval, and processing of images. In addition, new data storage techniques are needed to implement a practical memory.

The last three years of this research program have focused on (1) development of new phase modulation techniques to enhance the storage, retrieval, and integrity of the stored information; (2) experimental studies of image storage and phase conjugate retrieval; (3) image processing; and (4) practical holographic storage of images by using the hybrid time-frequency approach. Specifically, SRI demonstrated data encryption by phase modulating the read and write pulses. Image correlation and convolution was demonstrated and its implication for pattern recognition examined. Finally, this laboratory demonstrated high-fidelity random access and retrieval using holographic storage in $Pr^{3+}:YAlO_3$ with a single-frequency ring laser.

These experiments have clearly demonstrated the practical viability of TDOM with existing technology. In the next stage of the research, the performance issues such as bit-error-rates, signal-to-noise ratios, and laser stability need to be addressed.

14. SUBJECT TERMS
Stimulated photon echoes, optical memory, image processing, pattern recognition, phase conjugation

15. NUMBER OF PAGES
21 +Appendices

16. PRICE CODE

17. SECURITY CLASSIFICATION OF REPORT Unclassified	18. SECURITY CLASSIFICATION OF THIS PAGE Unclassified	19. SECURITY CLASSIFICATION OF ABSTRACT Unclassified	20. LIMITATION OF ABSTRACT UL

CONTENTS

INTRODUCTION

The inherent high bandwidth available with optical frequencies encourages the search for new optical processes and materials that will permit the utilization of the theoretical capability of optical processing of information. Rapid advances both in fiber-optic communications and in data storage have already occurred. Also, research on the fundamental components of optical processes is proceeding rapidly and giving added stimulus to the concept of all-optical systems for rapid, high-volume information processing applications such as communications, computers, and image analysis.

High-speed, high-capacity, random-access memories play an increasingly vital role in computers, telecommunications, image analysis, and other applications requiring large memory capacity and high read/write rates. Traditional memory approaches are based on long-lived magnetic polarization and on short-lived electronic logic circuits. The rapid progress in these technologies, leading to increasing storage density and data transfer rates, has facilitated the continuing explosive growth of computer capability.

For the past three years, SRI International has been investigating a new concept for fast, high-density optical information storage based on the stimulated photon echo, which results from constructive and destructive interference of the coherent emissions from a crystalline recording medium. Binary input data, represented by a sequence of short laser pulses, are recorded as modulations in the population distribution among the hyperfine levels of the ground state of the active atoms. The stored information is retrieved later by exciting the sample with a single laser pulse. The modulation in the ground state population is thus transferred to the excited state, where the regular pattern of the modulation results in temporal recurrence of constructive interferences between the emissions, leading to a train of emission pulses that reproduce the information stored.[1-6]

During the past three years, we have demonstrated a new storage scheme for time-domain optical memory (TDOM): it utilizes the pulse compression technique[5] originally developed for radar systems. In this scheme, the write and read pulses are biphase-modulated according to the Barker codes[5] to increase their bandwidth. We show that this approach to data storage possesses the same advantage as a frequency-chirped system, namely, the low laser-power requirements. In addition, this technique allows us to secure stored information, since identical coding for both write and read pulses is needed to recall faithfully the stored data.

1

The data throughput into and out of the memory can be increased substantially if the data pulses carry additional spatial information, namely, two-dimensional (2-D) images. This parallel storage approach using 2-D images has been demonstrated recently,[5,6] and the results showed there was no measurable effect on the write speed. Thus, a potential high-speed, high-density, page-oriented, all-optics memory is possible with the stimulated echo.

However, the quality of the retrieved images in the earlier demonstration[5,6] of stimulated echo image storage was generally very poor. No attempt was made to address issues regarding the intrinsic spatial resolution, the fidelity of the retrieved images, and the likely causes of various image distortions, for example. These issues are vital in evaluating TDOM, and we have addressed them in considerable detail during the last three years. Our objectives were to examine the quality of echo images under various experimental conditions by recording them with precision and to explore the significance of the results with regard to the future development of a working prototype.

Our work focused on examining the fidelity of the recalled images and their spatial resolution as well as various image processing operations offered by the memory. The recalled images were found to be of good quality because of their phase-conjugate nature. This unique feature motivated us to examine the feasibility of using fiber optics for image transmission—an issue important to the development of such a memory device. Two primary processing operations, two-image convolution and correlation, were demonstrated, and implications of the results for high-speed pattern recognition and optical interconnections are discussed in this report.

We have discovered a practical approach to image storage in a coherent time-domain optical memory that can be readily implemented with existing technologies. In this approach, 2-D images are stored holographically in narrow (≤ 1 MHz) frequency channels of a time-domain storage material, with one image per channel. Advantages of this approach include fast single-frame recording time, variable playback speeds, random frame access, and the ability to perform in-memory image processing. Experimental results have demonstrated high-resolution, high-fidelity, single-channel image storage in $Pr^{3+}:YAlO_3$ with the use of a single-frequency ring laser.

BACKGROUND

To illustrate the storage of information in the time domain, we use a simple diagram to describe the storage and retrieval of, first, a single bit, and then several bits, of information. Figure 1(a) shows the temporal sequence of laser pulses (i.e., the write, data, and read pulses) required to store and retrieve several bits of serial information. The frequency of the laser excitation pulses is fixed to a particular color that is in resonance with a particular group of atoms within the larger absorption line of the memory crystal. We use a rare-earth ion doped in a crystal as our memory crystal. At low temperatures (4 to 10 K), the width of the frequency absorption of a single rare-earth ion is very small (a few kilohertz). However, the overall absorption width of the memory crystal is much larger (many gigahertz) because the rare-earth ions occupy a distribution of different sites in a crystal. Therefore, individual ions do not see the write and data pulses occurring, respectively, at times $t_w = 0$ and t_D as two different pulses but rather as a complex pulse with a well-defined frequency Fourier transform.

For simplicity, Figure 1(b) shows the frequency Fourier transform (FT) of the write pulse and one of the data pulses from Figure 1(a). The FT of the three-pulse data pulse train shown in Figure 1(a) will be more complex than that shown in Figure 1(b). Figure 1(b) shows that the excitation spectrum is not uniform but is amplitude-modulated at frequencies proportional to the FT of the data pulse train. Therefore, the absorption of the memory crystal around the color of the laser itself will be modulated as a function of the absorption frequency. In other words, within a micron-sized pixel in the memory crystal, the serial bits representing information in the time domain are stored by a small group of atoms absorbing a particular color of light by Fourier transforming the temporal signal into frequency-domain absorption modulation. The information can be stored for many hours at low temperatures in a Eu^{3+}:$YAlO_3$ crystal.

To read the information, we need only excite the memory crystal at time t_R with a single laser pulse of the same colors as the data and write pulses. The read pulse causes the atoms to take the inverse Fourier transform of the frequency population modulation, and the result is a coherent emission or echo by the memory crystal at time $t_R + (t_D - t_W)$. The echo pulse emitted by the memory crystal mimics the data pulse train, and the serial data can therefore be retrieved. Furthermore, the coherent nature of the emitted signal from the memory crystal allows the entire signal to be captured by a single detector at a high signal-to-noise ratio.
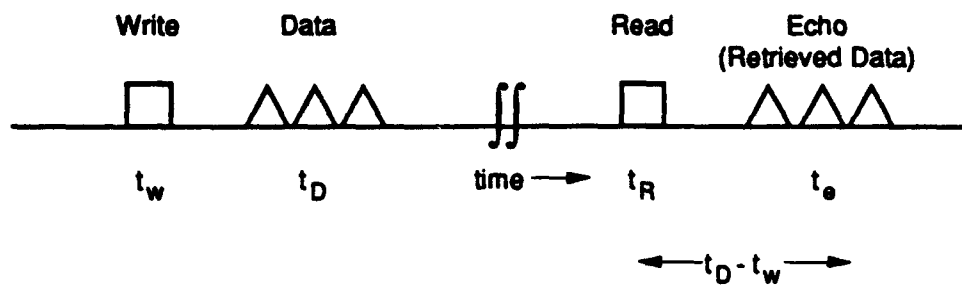
(a) Temporal sequence of laser pulses
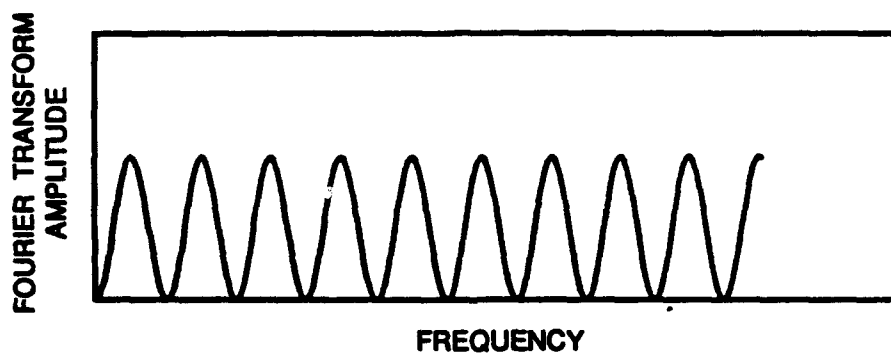
(b) Frequency Fourier transform of the write pulse
and a single data pulse shown in (a)

CAM-330581-5A

Figure 1. Storage and retrieval of information.

4

We can begin to evaluate the potential storage density and read/write speeds for the stimulated echo memory approach by considering the restrictions placed on the laser pulses by the spectral properties of the absorbing atoms. The first requirement is that the laser pulses be separated by enough time that they are distinguishable. The minimum temporal separation between neighboring pulses is given by

$$\tau_p = \frac{1}{\pi \delta_I}$$

where δ_I (called the inhomogeneous linewidth) is the spread in the absorption frequencies of the atoms in the various sites in the sample.

The second requirement is that the last data pulse must arrive while the excited atomic dipoles can still compare it with the first data pulse. The maximum time between the first and last data pulse is given by

$$T_2 = \frac{1}{\pi \delta_H}$$

where δ_H (called the homogeneous linewidth) is the effective absorption linewidth of an atom at a specific site. T_2 is also called the dephasing lifetime. Its maximum value is the radiative lifetime of the excited state.

Thus, T_2/τ_p (or equivalently, δ_I/δ_H) bits of information at most can be stored in a single spot, and the read/write rate is just $1/\tau_p$. For Eu^{3+} doped in Y_2SiO_5, the optimum storage material, the ratio δ_I/δ_H is 5×10^6 and $\tau_p = 100$ ps, resulting in a read/write rate of greater than 10^{10} bits/s and a storage density of more than 10^6 bits per spatial spot.[7]

RANDOM ACCESS MEMORY

As discussed in the preceding section, stimulated echo (SE) memory is a high-speed, dense optical memory and is intrinsically massively parallel. In the standard implementation of the SE memory, long word sizes in the range of 10^4 to 10^5 bits emerge in a natural way to achieve the high-density optical storage. The long word size is reasonable and perhaps desirable for some random mass memory applications. However, in contrast, random-access memory application requires partitioning the memory into smaller subunits so that each memory location has the following features:

(1) Word size should be smaller (16, 32, 64, 128... bits long), so that each memory location is randomly accessible for both reading and writing without other locations being affected.

(2) The contents of each memory location should, in principle, be independently erasable.

(3) Reading and writing to different memory locations simultaneously should be possible.

To address these random-access memory features, a new data storage scheme that is, in essence, a hybrid of the time-domain SE concept and the frequency-domain hole-burning scheme has been developed. The basic new idea is the partitioning of the absorption frequency domain into smaller bins, so that each frequency bin stores a smaller amount of information independently. The bins are distinguishable by their different absorption frequencies, and they are accessed by changing the laser frequency (color). However, information is still read and written using SE concept (i.e., the time-domain pulse sequence).

RESULTS

USE OF BIPHASE-CODED PULSES FOR WIDEBAND DATA STORAGE IN TIME-DOMAIN OPTICAL MEMORIES

We have demonstrated a new storage scheme for a time-domain optical memory: it utilizes the pulse compression technique[8] originally developed for radar systems. In this scheme, the write and read pulses are biphase-modulated according to the Barker codes[8] to increase their bandwidth. As discussed below, this approach to data storage possesses the same advantage as a frequency-chirped system, namely, the low laser-power requirements. In addition, this technique allows us to secure stored information, since identical coding for both write and read pulses is needed to recall faithfully the stored data.

The use of phase-modulated pulses to perform data storage and retrieval in a time-domain optical memory was first investigated by Zhang et al.[9] These authors introduced pseudo-random-phase noise to the write and read pulses in an attempt to increase the bandwidth of the pulses. However, the signal-to-noise ratio of their retrieved data was poor. In this demonstration, instead of random-phase noise, we used the 13-bit Barker code to biphase-modulate the write and read pulses. This modulation effectively divides a long pulse of duration T into N (i.e., 13 here) subpulses of equal length τ, whose phase either remains unchanged or is shifted by π. Several important properties of the Barker codes (also known as "perfect" codes) are worth mentioning here. An autocorrelation of such a code yields a compressed pulse and some sidelobes.[8] The compressed peak occurs at the center of the correlation function and expands over a time duration of 2T. The energy among the sidelobes is uniformly distributed. Furthermore, the electric field envelope of the compressed pulse has a triangular shape with a width (full width at half maximum, FWHM) of τ. Finally, the ratio of the compressed peak intensity to the maximum sidelobe power is equal to N^2 (Ref. 10). For the 13-bit Barker code, this ratio is 169.

The experimental setup used to demonstrate the faithful storage and retrieval of optical information by using biphase-modulated pulses is shown in Figure 2, along with the temporal sequence of the laser and echo pulses. An experimental setup is described in detail in Appendix A. Five data pulses with different lengths and intensities were used to examine the faithfulness of the data retrieval. These pulses, along with the write and read pulses, were focused into the $Pr^{3+}:YAlO_3$ crystal as shown in Figure 2. The laser spot size at the sample was measured to be

approximately 125 μm (FWHM). The separation between the write pulse and first data pulse ($t_d - t_w$) and that between the first data pulse and the read pulse ($t_r - t_d$) were approximately 4 and 19 μs, respectively. With this arrangement, the echo pulse train started 4 μs after the arrival of the read pulse.
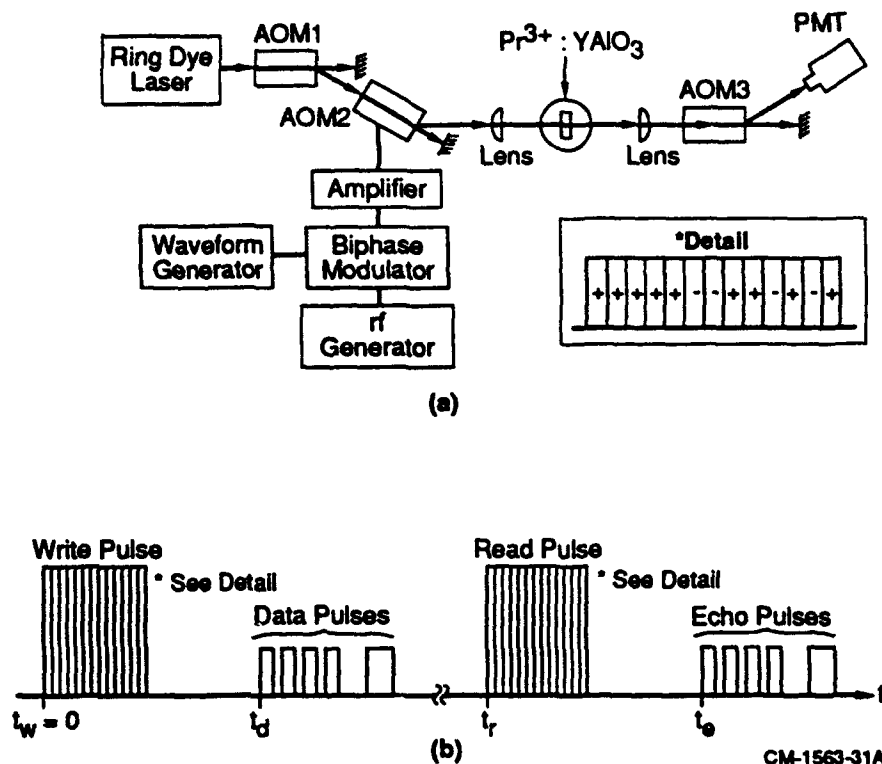

Figure 2. Experiment to demonstrate the use of biphase-coded write and read pulses for the storage and retrieval of optical data in a stimulated echo memory. (a) Schematic of experimental setup. AOMs, acousto-optical modulators; PMT, photomultiplier tube. (b) Temporal sequence of the laser and echo pulses. The write and read pulses were biphase-modulated as shown by the + and - signs. The + sign represents no phase change, while the - sign represents a phase shift of π radians.

8

Figure 3 shows experimental results demonstrating the storage and retrieval of 5-bit optical data with the 13-bit Barker code. In Figure 3(a), the write and read pulses had identical coding and, as expected, the stored data were faithfully recalled. The fact that the intensity of the third input data pulse was higher than the rest was clearly reflected in the echo signal recorded here. The slight intensity modulation of the echo pulses was in part due to the presence of hyperfine splitting of the $^1D_2$ state of Pr^{3+}, which can be removed by choosing appropriate rare-earth solids, (e.g, Eu^{3+} doped materials). Here the width of the first four pulses was approximately 300 ns while that of the fifth pulse was 600 ns. Because the first four pulses were not significantly longer than the compressed pulse (~125 ns) resulting from the autocorrelation, the effect of subsequent convolution with the data pulses is evident, that is, the shape of the first four recalled pulses is nearly triangular instead of rectangular [see Figure 3(a)]. Our estimate of the sidelobe-induced background intensity relative to the recalled data pulse intensity for the data pulse train used here indicates the signal-to-background ratio to be ~10, in good agreement with the experimental results.

To demonstrate the technique's ability to secure stored data, we purposely changed the coding of the read pulse so that the write and read pulses were not identical. Figure 3(b) shows the results obtained with the mismatched write and read pulses. Here the 11th and 13th bits of the read pulse were incorrectly coded. As a result, the recalled echo signal did not resemble the input data. The fine structures observed in the write and read pulses in Figure 3 were caused by the biphase modulation. Here the data were obtained by averaging over 64 events at a rate of 30 Hz, and the energies of the write and read pulses used were ~50 nJ.

Unfortunately, the longest known Barker code has only 13 bits, which limits[8] the time-bandwidth product of such codes to no more than 13. However, there do exist longer codes[11] (known as "good" codes), whose sidelobe structures are nearly uniform. In addition, polyphase codes[12] can also be used to increase the time-bandwidth product to permit the storage of ultrashort data pulses with long write and read pulses.

IMAGE STORAGE AND RETRIEVAL THROUGH AN OPTICAL FIBER

Image information, encoded as a spatial intensity pattern, is rapidly scrambled as it propagates in an optical fiber because of mode coupling.[13] The only method known thus far to restore an image scrambled by an optical fiber is to use a phase-conjugating mirror and retransmit the scrambled image through an identical fiber link. This finding limits the practical use of optical fibers for image transmission.
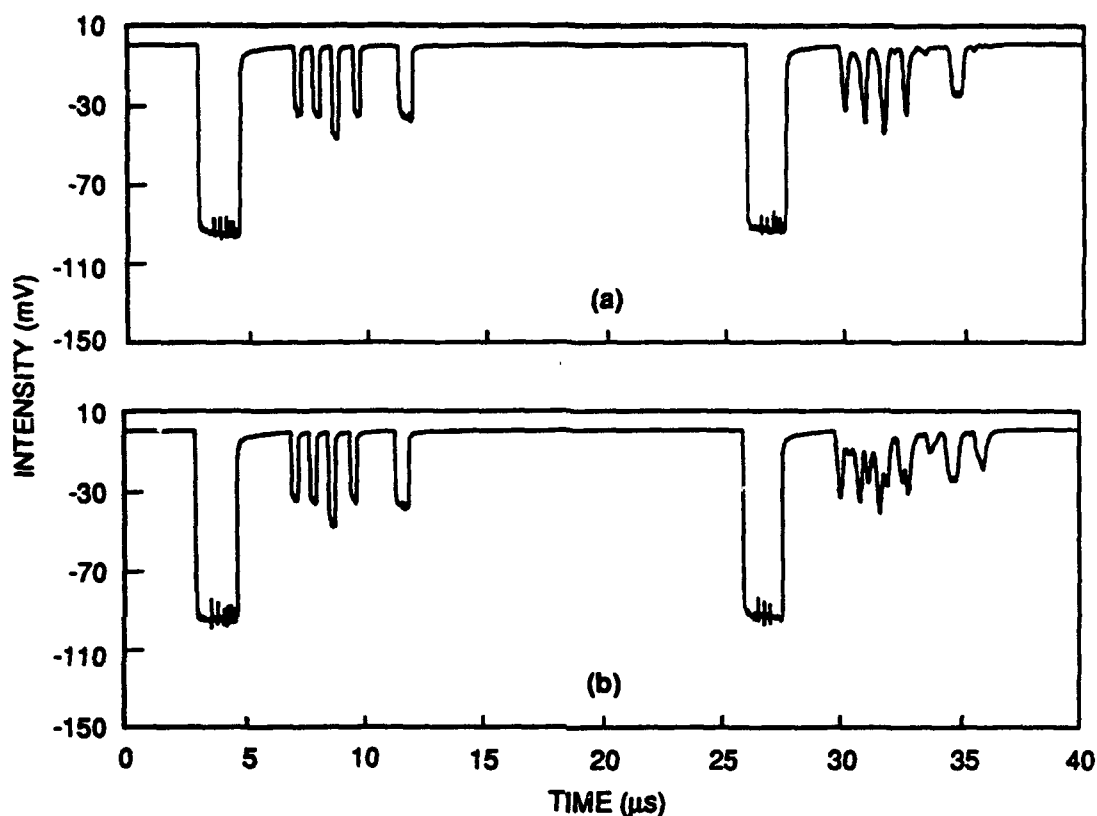
Figure 3. Storage and retrieval of 5 data pulses using biphase-coded write and read pulses. (a) Here the write and read pulses were coded identically by using the 13-bit Barker code. (b) Here 2 of the 13 bits (Bits 11 and 13) in the read pulse were coded incorrectly.

We present here an example in which optical fibers are used for image transmission in a practical image storage device. As discussed earlier, if the first input pulse is used as a data pulse, the time-domain optical memory is essentially a delayed phase-conjugating mirror. Therefore, the scrambled echo images, after being transmitted through the same fiber that creates the distortion during the data storage, are restored to their original, undisturbed form upon retrieval.

10

Figure 4 shows experimental results demonstrating such an application for image transmission. A detailed description of the experimental apparatus is included in Appendix B. Here the input image was first focused into a multimode fiber (400 μm in diameter, 40 cm long) by using a 400-mm focal length lens. The output from the fiber was then imaged onto the sample (see the part labeled "Optional" in Figure 1 of Appendix B). As expected, the input image was completely scrambled after being transmitted through the fiber [Figure 4(b)]. However, when the scrambled image was stored and later retrieved through the same fiber, we detected a restored image, as shown in Figure 4(c).

(a)   (b)   (c)
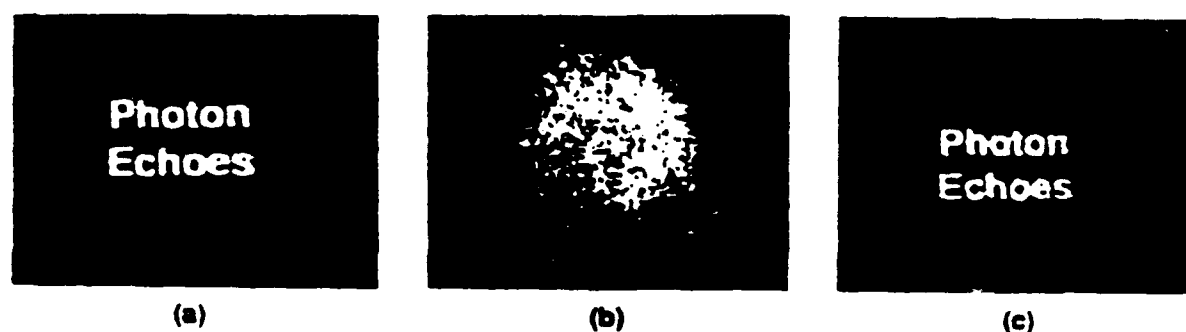
CPM 1563 24

Figure 4. Experimental demonstration of phase conjugation. (a) Input data image, (b) after passage through a multimode optical fiber, and (c) echo image retrieved.

These results have important implications for the development of TDOM. With optical fibers, the memory can be more compact and requires no optical alignment. Furthermore, multiple fibers can be used to simultaneously store and retrieve many images and thus increase further the data throughput rate or to store large images that cannot be handled by lens systems. Another potential application of this fiber-based optical memory would be a multiuser central system, where each user's data are stored through an optical fiber in one memory location in the central system. This approach would significantly reduce the cost as well as the effort of keeping the storage material at required low temperatures. However, issues such as the effect of fiber thermal fluctuation on retrieved images must be carefully studied before this technique is implemented.
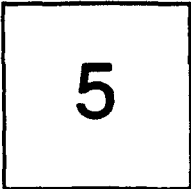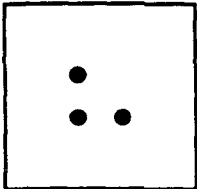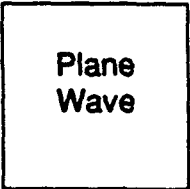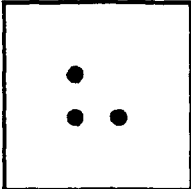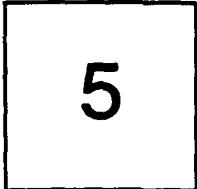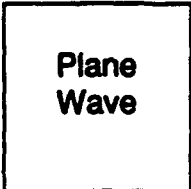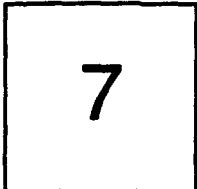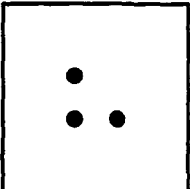
HIGH-SPEED IMAGE PROCESSING

The unique storage/retrieval mechanism of TDOM permits its use for high-speed image processing as discussed earlier. Xu et al. have demonstrated the operation of two-image correlation using TDOM.[14] However, because these authors used transmission masks with high degrees of symmetry, they were unable to demonstrate certain features of spatial correlation. In addition, two-image convolution available with TDOM has not previously been studied experimentally.

To demonstrate two-image convolution and correlation with clarity, we used transmission masks with low degrees of symmetry, such as the numerals "5" and "7". The horizontal direction (from left to right) of the masks was chosen to be the X-axis and the vertical direction (from bottom to top) to be the Y-axis. The Z-axis (using the right-hand coordinate system) was chosen to be along the same direction as that of the second (write) pulse. Our experimental results (summarized in Figure 5) show that the two-image correlation operations [Figures 5(a) and (b)] are not symmetric with respect to the order of the inputs, but the convolution operations are [Figures 5(c) and (d)]. Figure 5 further shows that if the second pulse were used as a data pulse, the retrieved image would be inverted ($x \rightarrow -x$, $y \rightarrow -y$), as predicted by Relation (2) in Appendix C.

This demonstrated processing ability, along with the potentially high storage density, makes TDOM an ideal candidate for high-speed pattern recognition. A large data base can be created before processing by storing reference images into the memory sequentially, using a single write pulse. The unknown spatial information to be analyzed (or the data image) is carried by the read pulse at a later time. Under this condition, the echoes generated upon the arrival of the data image are the spatial correlations between the data image and ev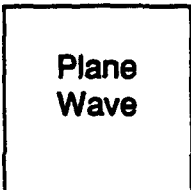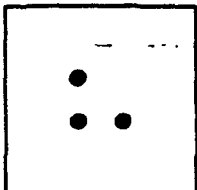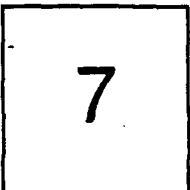ery reference image. Since the temporal sequence of the echo pulses is uniquely related to that of the reference pulses, the reference image that yields high spatial correlation with the data image can then be identified from the corresponding echo image. Such an application to pattern recognition has recently been demonstrated successfully in our laboratory.[15]

Further applications of TDOM include optical interconnects, where the stored images can be directed simultaneously to many output ports by using an appropriately encoded read pulse. Figure 5(c) demonstrates such an application, where the stored numeral "7" was sent simultaneously to three output ports by the read pulse. The advantage of this approach for optical interconnects is its rapid reprogrammability. The output ports can be changed every time a read command is issued.

12

	Input Images			**Echo Image**
	1	2	3	

Figure 5.   Experimental results showing the use of TDOM to perform (a)-(b) two-image
correlations and (c)-(d) two-image convolutions.

13

TIME-DOMAIN HOLOGRAPHIC IMAGE STORAGE

We have invented a new approach to time-domain image storage. This approach not only retains those features that are unique to CTDOM but also permits random frame access and variable playback speed. Most importantly, it can be readily implemented with the use of existing low-power cw lasers, a key requirement for a practical storage device.

In the proposed approach, two-dimensional input images are stored in narrow ($\Delta v \leq 1$ MHz) frequency channels within an inhomogeneously broadened absorption line of a rare-earth solid by using a low-power cw laser, with one frame per frequency channel (Figure 6). Each image is stored by first tuning the laser wavelength to the desired channel and illuminating the sample with two temporally separated pulses known as the reference (E_{r_1}) and the object (E_o) pulses. E_{r_1}, a spatially uniform laser pulse carrying no information, proceeds E_o, which carries the spatial information (e.g., an image) to be stored. The latter can be generated by transmitting a spatially uniform laser pulse through a spatial-light-modulator (SLM). The image thus recorded is a time-domain hologram resulting from the interference of the temporally delayed pulses via interaction with dipoles in the storage material.

The above recording procedure is repeated for subsequent input images at different channels, and it can be initiated, for example, at the low-frequency side of the inhomogeneous line and completed at the opposite side by incrementally increasing the laser wavelength at the corresponding input rate. For an inhomogeneous bandwidth of 6 GHz (typical of a rare-earth solid) and $\Delta v = 1$ MHz, a total of 6000 images can be stored at one spatial location.

The image stored in a particular channel is recalled by tuning the laser wavelength to the channel location and exciting the sample with another reference pulse (or the read pulse, E_{r_2}), whose spatial profile is identical to that of E_{r_1}. The read pulse induces an echo that contains spatial information identical to E_o.

The time required to record a single frame, τ_s, is determined by the temporal widths of E_{r_1} and E_o as well as their separation, which can be reduced to zero with no effect on the stored information. The channel switching time can be much shorter than τ_s for the small frequency increment proposed here (i.e., ≤ 1 MHz). Thus, the upper limit of the recording speed is determined mainly by the reciprocal of τ_s, and the latter can be estimated from the efficiency of a stimulated echo.

To demonstrate the feasibility of using low-power lasers for image storage in the proposed scheme, we performed two-dimensional image storage in a $Pr^{3+}:YAlO_3$ crystal (~0.1 at.%).

14
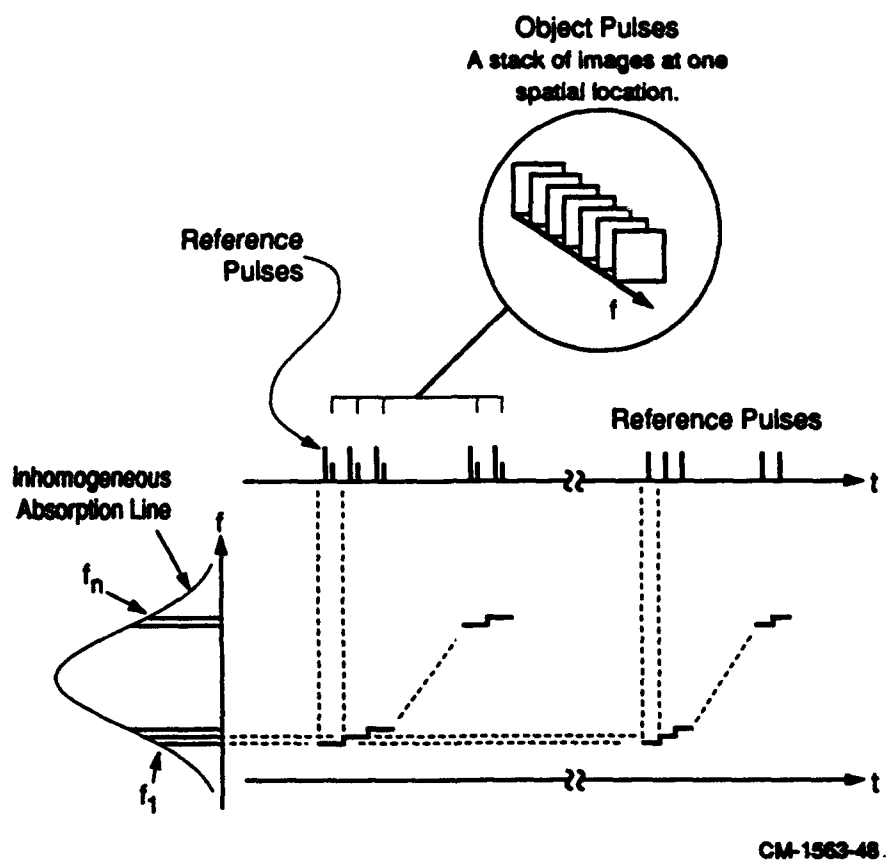
Figure 6. Schematic of the one-frame-per-channel approach to image storage in CTDOM.

Figure 7 shows the schematic of the experimental apparatus (see Appendix D). The $^3H_4$-$^1D_2$ transition of Pr^{3+}:$YAlO_3$ (a wavelength of 610.5 nm) was used, and the sample (2.5 mm thick × 7-mm diameter) was mounted in a He-vapor cryostat at ~4 K. The arrangement of E_o and E_{r_1} (E_{r_2}) here was chosen to be similar to arrangements used in standard holographic data storage, i.e., E_o and E_{r_1} (E_{r_2}) propagate along different directions and intersect at the sample as shown in Figure 7 (here the intersecting angle was ~8°). Instead of imaging the input on the sample to the size required for efficient echo generation, we used a single lens and placed it behind the mask to focus the image down to approximately 1 × 1 mm. An identical lens was used behind the sample to reconstruct the focused image back to its original form, which was then detected by a gated intensified charged-coupled-device (CCD) camera (a 6 × 4.5 mm CCD chip with 610 × 488 pixels). The separation between the mask and focusing lens was chosen to be equal to the focal length. The image thus stored was only an approximate Fourier image (because the sample was not exactly in the focal plane) and therefore, to prevent image-dependent saturation at the center, its DC terms were spread over a much larger area than for an exact Fourier image.
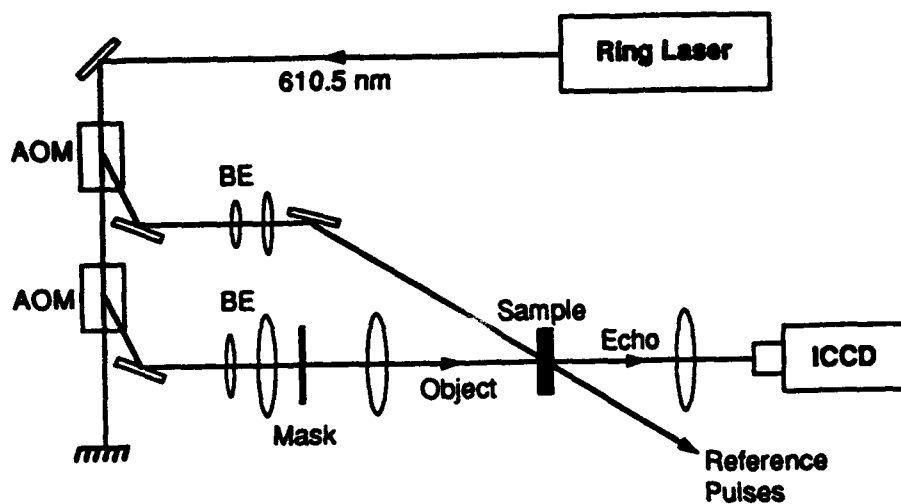
CM-1563-47

Figure 7. Experimental setup for time-domain holographic image storage. AOM, acousto-optic modulator; ICCD, intensified CCD camera; BE, beam expander.

16

Figure 8 shows an input (a standard U.S. Air Force resolution chart) and its echo image. The image was stored by a 5-μs-long reference pulse and later recalled by a read pulse of the same length. For experimental convenience, we chose the separation between E_{r_1} and E_0 (or E_{r_2}) to be ~15 μs (or 55 μs) and the length of E_0 to be 2.5 μs. The power of the three inputs was ~150 mW. Careful inspection shows that the closest line pairs resolved were >4.0 line pairs/mm (group 2, element 1). The echo image was obtained from a single storage/retrieval event with no signal averaging.

We further examined the response of echoes to grayscale inputs by using a mask (4 × 11 mm) consisting of six different transmission levels [Figure 9(a)]; the recorded echo is shown in [Figure 9(b)]. To quantitatively evaluate the image quality, we plotted [Figure 9(c)] the intensity averaged over rows (excluding the rows where numeric labels for different brightness bands were located) as a function of the column number for both the object and echo images; we found that the brightness ratios taken between adjacent transmission levels of the echo match those of the object image to within 13%. The observed low intensity in the first 40 columns in [Figure 9(c)] arises from the presence of opaque letters printed along the side of the input, and the slow change of intensity from one brightness level to the next is caused by slight misalignment of the input image with respect to the CCD camera.

(a)   (b)
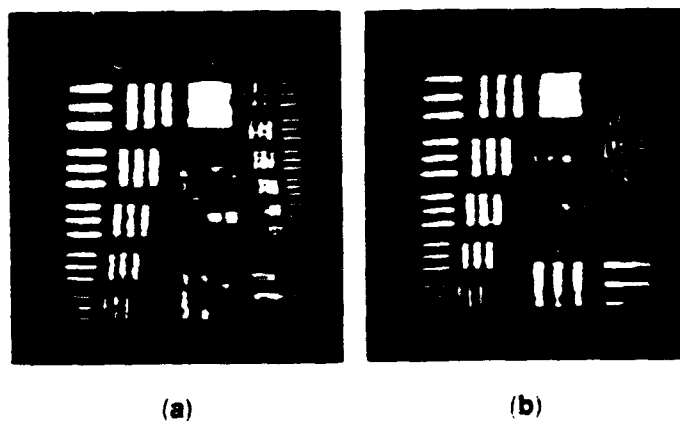
CP-1563-45

Figure 8. Experimental results demonstrating holographic image storage in CTDOM.
(a) Input image (resolution chart), (b) echo image.

(a)

(b)

(c)
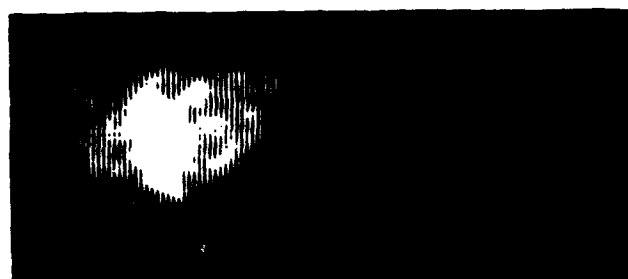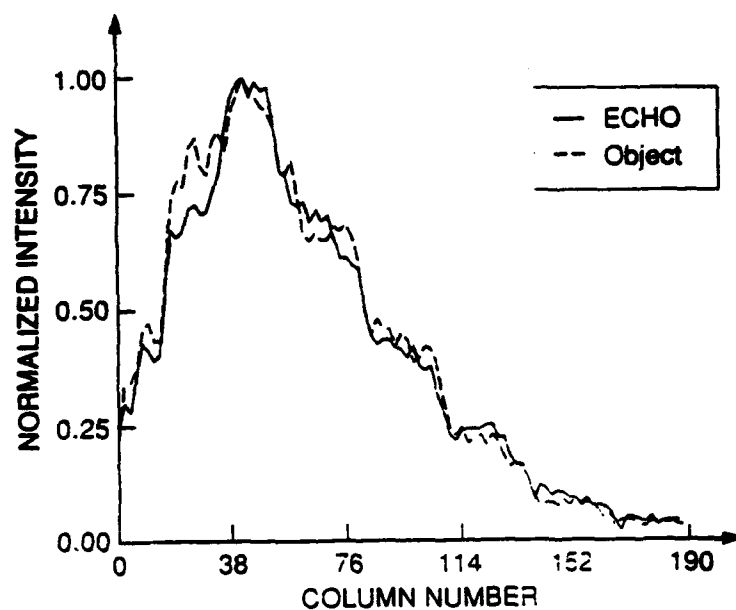
CP-1563-46A

Figure 9. Experimental results demonstrating the storage of grayscale inputs. (a) Input image consisting of six different transmission levels. (b) Recalled image. (c) Average intensities of the input and echo as a function of the column number.

18

The quality of the recorded images here (both the input and the echoes) was found to be limited by the nonuniform response of the gated image intensifier in the CCD camera. Images (e.g., input images) with improved quality can be obtained by using a conventional CCD camera having no microchannel-plate intensifier. This finding suggests that the intrinsic quality of the echo images may well be higher than what was observed here. Another factor affecting the image quality is the Gaussian nature of laser spatial profiles. Spatially uniform laser beams are necessary for high-quality image storage.

CONCLUSIONS

We have successfully demonstrated that appropriately phase-coded laser pulses can replace frequency-chirped pulses to perform data storage and retrieval in a time-domain optical memory. The advantage of this approach is that it also provides a means of securing the stored information. Without a detailed knowledge of the coding used for the write pulses, the stored information cannot be recalled faithfully.

We have examined the use of the time-domain optical memory for image storage and image processing. Our results suggest the first pulse should be used as a data pulse to carry spatial information for image storage, since under this condition the retrieved image is the phase-conjugate replica of the data image. This unique feature not only ensures the recall of distortion-free images but also permits the use of optical fibers for image transmission. The latter property opens up the possibility of developing fiber optics-based image storage devices.

The inherent image processing capability of TDOM provides unprecedented flexibility in handling stored information and makes TDOM an ideal candidate for high-speed pattern recognition and optical interconnections. Combining these features with the temporal processing ability demonstrated elsewhere, TDOM shows an incomparable potential to be a high-performance, high-density, massively parallel optical memory with features such as content-based retrieval.

We have devised a practical approach to image storage in TDOM that features random frame access, variable high recording and playback speeds, and in-memory image processing. A feasibility study of this approach was undertaken by storing a single image into a 1-MHz-wide frequency bin. The stored image had good spatial quality and high fidelity.

20

REFERENCES

1. T. W. Mossberg, A. Flussberg, R. Kachru, and S. R. Hartmann, Phys. Rev. Lett **42**, 1665 (1979).

2. R. Kachru, T. W. Mossberg, and S. R. Hartmann, Opt. Commun. **30**, 57 (1979).

3. T. W. Mossberg, Opt. Lett. **7**, 77 (1982).

4. N. W. Carlson, W. R. Babbitt, and T. W. Mossberg, Opt. Lett. **8**, 623 (1983).

5. M. K. Kim and R. Kachru, J. Opt. Soc. Am. **134**, 305 (1987).

6. M. K. Kim and R. Kachru, Opt. Lett. **12**, 593 (1987).

7. Y. S. Bai and R. Kachru, Opt. Lett. **18**, 1189 (1993).

8. M. N. Cohen, in *Principles of Modern Radar*, J. L. Evans and E. K. Ready, Eds. (Van Nostrand Reinhold, New York, 1987), and references therein.

9. J. M. Zhang, D. J. Gauthier, J. Huant, and T. W. Mossberg, Opt. Lett. **16**, 103 (1991).

10. X. A. Shen, Y. S. Bai, and R. Kachru, Opt. Lett. **17**, 1079 (1992).

11. J. Lindner, Electron. Lett. **11**, 507 (1975).

12. S. W. Golomb and R. A. Scholtz, IEEE Trans. **IT-11**, 533 (1965).

13. A. Yariv, Appl. Phys. Lett. **28**, 88 (1976).

14. E. Y. Xu, S. Kroll, D. L. Huestis, and R. Kachru, Opt. Lett. **15**, 562 (1990).

15. X. A. Shen and R. Kachru, Opt. Lett. **17**, 520 (1992).

Appendix A

USE OF BIPHASE-CODED PULSES FOR WIDEBAND DATA STORAGE IN TIME-DOMAIN OPTICAL MEMORIES

Use of biphase-coded pulses for wideband data storage in time-domain optical memories

X. A. Shen and R. Kachru

We demonstrate that temporally long laser pulses with appropriate phase modulation can replace either temporally brief or frequency-chirped pulses in a time-domain optical memory to store and retrieve information. A 1.65-μs-long write pulse was biphase modulated according to the 13-bit Barker code for storing multiple bits of optical data into a Pr^{3+}:$YAlO_3$ crystal, and the stored information was later recalled faithfully by using a read pulse that was identical to the write pulse. Our results further show that the stored data cannot be retrieved faithfully if mismatched write and read pulses are used. This finding opens up the possibility of designing encrypted optical memories for secure data storage.

Key words: Stimulated photon echoes, time-domain optical memory, Barker codes, biphase pulse compression.

The use of stimulated echoes for storing optical information in rare-earth solids has received increased attention in recent years.[1,2] The technique (referred to as the time-domain optical memory) has shown the potential of providing high storage density and high read–write speed simultaneously. Additional features, such as the ability to perform in-memory signal processing,[3,4] also make the stimulated echo an ideal candidate for high-speed digital and analog signal processing. Two storage schemes have been developed: one uses temporally brief write and read pulses for storing and recalling optical data,[5] and the other uses temporally long frequency-chirped pulses.[6] The latter approach was found to be more practical since it requires substantially lower power for the write and read pulses and yet provides the bandwidth needed to handle short data pulses.

Here we propose and demonstrate a new storage scheme for a time-domain optical memory, which uses the pulse compression technique[7] originally developed for radar systems. In this scheme the write and read pulses are biphase modulated according to the Barker codes[7] for increasing the pulse bandwidth. We show that this approach to data storage possesses the same advantage as a frequency-chirped system,

namely, low laser-power requirements. In addition, this technique permits us to secure stored information since identical coding for both write and read pulses is needed to recall faithfully the stored data.

The use of phase-modulated pulses for performing data storage and retrieval in a time-domain optical memory was first investigated by Zhang *et al.*[8] These authors introduced pseudorandom-phase noise to the write and read pulses in an attempt to increase the bandwidth of the pulses. However, the signal-to-noise ratio of their retrieved data was poor. In this demonstration, instead of random-phase noise, we used the 13-bit Barker code to biphase modulate the write and read pulses. This modulation effectively divides a long pulse of duration T into N (i.e., 13 here) subpulses of equal length τ, whose phase either remains unchanged or is shifted by π. Several important properties of the Barker codes (also known as perfect codes) are worth mentioning here. An autocorrelation of such a code yields a compressed pulse and some sidelobes.[7] The compressed peak occurs at the center of the correlation function, which expands over a time duration of $2T$. The energy among the sidelobes is uniformly distributed. Furthermore, the electric-field envelope of the compressed pulse has a triangular shape with a width (FWHM) of τ. Finally, the ratio of the compressed peak intensity to the maximum sidelobe power is equal to N^2. For the 13-bit Barker code this ratio is 169.

The use of the biphase-coded pulses for storing and retrieving optical data can be appreciated by examining the following expression[6] for the stimulated-echo

A-1

electric-field envelope in a small pulse area limit:

$$E_e(t) \propto \int_{-\infty}^{+\infty} E_w^*(\omega)E_d(\omega)E_r(\omega)\exp(-i\omega t)d\omega. \quad (1)$$

Here $E_w(\omega)$, $E_d(\omega)$, and $E_r(\omega)$ are the Fourier transforms of the electric-field envelopes of the write, data, and read pulses, respectively. The above relation can be rewritten in terms of correlation and convolution among the pulses:

$$E_e(t) \propto [E_w(t'') \otimes E_r(t'')] * E_d(t'), \quad (2)$$

where $\otimes$ and $*$ represent the temporal correlation and convolution, respectively. It is clear from Eq. (2) that, in order to retrieve faithfully E_d (i.e., $E_e \propto E_d$), one requires the correlation of E_w with E_r to be a single sharp peak with a temporal width much shorter than the shortest data pulses of interest.

The compression of pulses through a correlation operation, as discussed earlier, can be achieved by using the Barker codes. For example, the width of the compressed peak obtained from the autocorrelation of a 13-bit Barker code is only 1/13 of that of the input, while the intensity of the peak is 169 times higher than the maximum power of the sidelobes. Thus one can neglect the sidelobes in the subsequent convolution with data pulses, provided that (a) the data bandwidth is smaller than the bandwidth of the write–read pulses (i.e., $1/\tau$) and (b) the individual data pulse length is much shorter than the total length of the sidelobes (i.e., $2T$). The latter requirement arises because of the particular Barker code used here. The sidelobes generated by the autocorrelation of the 13-bit code happen to have an identical phase. Thus their convolution with a long pulse ($\geq 2T$) would lead to the integration of all the sidelobes, giving rise to a high background level. However, this pulse-length requirement can be removed if the data-pulse train is biphase modulated at a rate of $1/\tau$. We have successfully demonstrated recently the use of the Barker codes for compressing optical pulses in a stimulated echo experiment.[4]

The experimental setup for demonstrating the faithful storage and retrieval of optical information with biphase-modulated pulses is shown in Fig. 1 along with the temporal sequence of the laser and echo pulses. The optical information was stored in a Pr^{3+}:$YAlO_3$ crystal (0.1 at. %) on the $^3H_4$–$^1D_2$ transition (transition wavelength of 610.5 nm) of the Pr^{3+} ions. The sample was mounted in a flowing helium vapor cryostat at a temperature of ~ 3.5K. A Coherent (model 699-29) single-frequency ring laser, along with an acousto-optic modulator (AOM2), was used to generate the write, data, and read pulses. The write and read pulses were phase modulated according the 13-bit Barker code. This modulation was accomplished at the rf level by using a biphase modulator, which in turn modulated the phase of the optical pulses.[9] The width of the subpulses resulting from this modulation was ~ 125 ns.

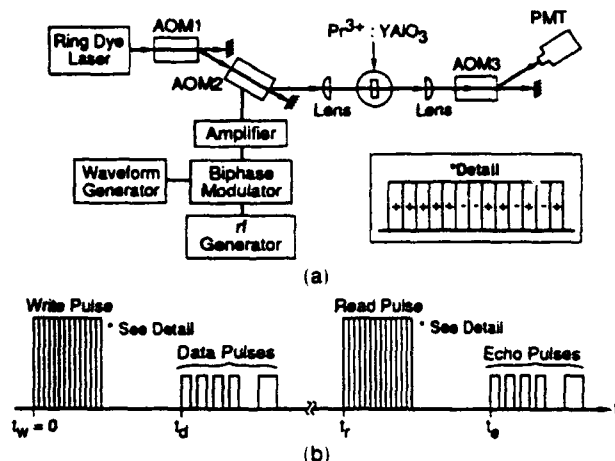Five data pulses with different lengths and intensi-

(a)

(b)

Fig. 1. (a) Schematic of experimental setup for demonstrating the use of biphase-coded write and read pulses for the storage and retrieval of optical data in a stimulated-echo memory: AOM1–AOM3, acousto-optical modulators; PMT, photomultiplier tube. (b) Temporal sequence of the laser and echo pulses. The write and read pulses were biphase modulated, as shown by the + and − signs. The + sign represents no phase change, while the − sign represents the phase shift π.

ties were used to examine the faithfulness of the data retrieval. These pulses, along with the write and read pulses, were focused into the Pr^{3+}:$YAlO_3$ crystal, as shown in Fig. 1. The laser spot size at the sample was measured to be ~ 125 µm (FWHM). The separations between the write and the first data pulses ($t_d - t_w$) and between the first data and read pulses ($t_r - t_d$) were approximately 4 and 19 µs, respectively. With this arrangement, the echo-pulse train started 4 µs after the arrival of the read pulse.

An additional acousto-optic modulator (AOM1) was employed to remove the residual dc signal caused by the insufficient extinction ratio of AOM2. This modulator produced a single pulse that was long enough for AOM2 to generate the required write, data, and read pulses, and it was turned off thereafter to minimize the dc background at the echo time. The modulator AOM3 in Fig. 1 served as a fast shutter to deflect only the echo pulses to the photomultiplier tube (PMT) for recording.

Figure 2 shows experimental results demonstrating the storage and retrieval of 5-bit optical data with the 13-bit Barker code. In Fig. 2(a) the write and read pulses had identical coding and, as expected, the stored data were faithfully recalled. The fact that the intensity of the third input data pulse was higher than the rest was clearly reflected in the echo signal recorded here. The slight intensity modulation of the echo pulses was in part caused by the presence of hyperfine splitting of the $^1D_2$ state of Pr^{3+}, which can be reduced at the rate of our experiment by choosing appropriate rare-earth solids (e.g., Eu^{3+}-doped materials). Here the width of the first four pulses was ~ 300 ns, while that of the fifth pulse was 600 ns. Because the first four pulses were not significantly longer than the compressed pulse (~ 125 ns) resulting from the autocorrelation, the effect of subsequent
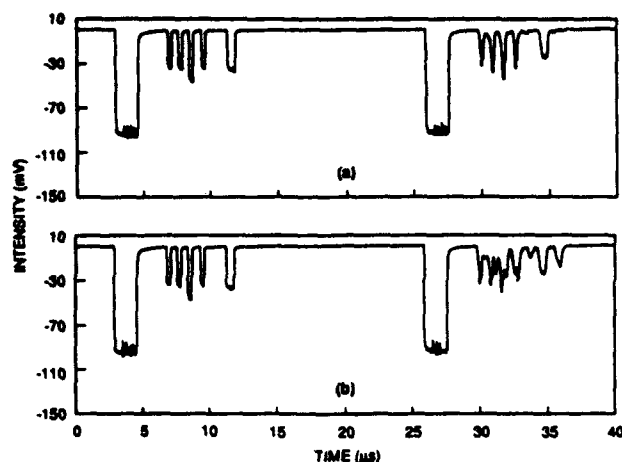
A-2

Fig. 2. Storage and retrieval of five data pulses with biphase-coded write and read pulses: (a) write and read pulses were coded identically by using the 13-bit Barker code, (b) two of the 13 bits (bits 11 and 13) in the read pulse were coded incorrectly.

convolution with the data pulses is evident; i.e., the shape of the first four recalled pulses is nearly triangular instead of rectangular [see Fig. 2(a)]. We estimated the sidelobe-induced background intensity relative to the recalled data pulse intensity for the data-pulse train used here, and we found the signal-to-background ration to be ~10, in good agreement with the experimental results.

To demonstrate the technique's ability to secure stored data, we purposely changed the coding of the read pulse so that the write and read pulses were not identical. Figure 2(b) shows the results obtained with the mismatched write and read pulses. Here the 11th and 13th bits of the read pulse were incorrectly coded. As a result, the recalled echo signal did not resemble the input data. The fine structures observed in the write and read pulses in Fig. 2 were caused by the biphase modulation. The data in Fig. 2 were obtained by averaging over 64 events at a rate of 30 Hz as the laser frequency was slowly swept (to avoid detecting accumulated echoes). The energies of the full write–read pulses used in both cases were ~50 nJ.

Unfortunately, the longest known Barker code has only 13 bits, which limits the time–bandwidth product of such codes to be no more than 13.[7] However, there do exist longer codes[10] (known as good codes), whose sidelobe structures are nearly uniform. In

addition, polyphase codes[11] can also be used to increase the time–bandwidth product for permitting the storage of ultrashort data pulses with long write and read pulses.

In conclusion, we have successfully demonstrated that appropriately phase-coded laser pulses can replace frequency-chirped pulses for performing data storage and retrieval in a time-domain optical memory. The advantage of this approach is that it also provides a means of securing the stored information. Without detailed knowledged of the coding used for the write pulses, the stored information cannot be recalled faithfully, as was demonstrated here.

References

1. S. Kröll, L. E. Jusinski, and R. Kachru, "Frequency-chirped copropagating multiple-bit stimulated-echo storage and retrieval in Pr^{3+}:$YAlO_3$," Opt. Lett. 16, 517–519 (1991), and references therein.

2. M. Mitsunaga, R. Yano, and N. Uesugi, "Time- and frequency-domain hybrid optical memory: 1.6-kbit data storage in Eu^{3+}:Y_2SiO_5," Opt. Lett. 16, 1890–1892 (1991), and references therein.

3. Y. S. Bai, R. Babbitt, N. W. Carlson, and T. W. Mossberg, "Real-time optical waveform convolver/cross correlator," Appl. Phys. Lett. 45, 714–716 (1984).

4. X. A. Shen, Y. S. Bai, and R. Kachru, "Reprogrammable optical matched filter for biphase-coded pulse compression," Opt. Lett. 17, 1079–1081 (1992).

5. M. K. Kim and R. Kachru, "Many-bit optical data storage using stimulated echoes," Appl. Opt. 28, 2186–2189 (1989).

6. Y. S. Bai, W. R. Babbitt, and T. W. Mossberg, "Coherent transient optical pulse-shape storage/recall using frequency-swept excitation pulses," Opt. Lett. 11, 724–726 (1986).

7. M. N. Cohen, in Principles of Modern Radar, J. L. Eaves and E. K. Reedy, eds. (Van Nostrand Reinhold, New York, 1987), pp. 465–501, and references therein.

8. J. M. Zhang, D. J. Gauthier, J. Huang, and T. W. Mossberg, "Use of phase-noisy laser fields in the storage of optical pulse shapes in inhomogeneously broadened absorbers," Opt. Lett. 16, 103–105 (1991).

9. A. Yariv, Quantum Electronics, 2nd ed. (Wiley, New York, 1975), pp. 327–370.

10. J. Lindner, "Binary sequences up to length of 40 with best possible autocorrelation function," Electron. Lett. 11, 507 (1975).

11. S. W. Golomb and R. W. Scholtz, "Generalized Barker sequences," IEEE Trans. Inf. Theory IT-11, 533–537 (1965).

A-3

Appendix B

**TIME-DOMAIN OPTICAL MEMORY FOR IMAGE
STORAGE AND HIGH-SPEED IMAGE PROCESSING**

Time-domain optical memory for image storage and high-speed image processing

X. A. Shen and R. Kachru

We present an experimental study on the use of the time-domain optical memory for image storage and high-speed image processing. We focus on examining the fidelity of the recalled images and their spatial resolution as well as various image-processing operations offered by the memory. The recalled images were found to be of good quality because of their phase-conjugate nature. This unique feature further motivated us to examine the feasibility of fiber optics being used for image transmission, an issue important to the development of such a memory device. Two primary processing operations, two-image convolution and correlation, were demonstrated, and implications of the results for high-speed pattern recognition and optical interconnections are discussed.

Key words: Stimulated photon echoes, time-domain optical memory, phase conjugation, two-image convolution and correlation.

1. Introduction

Optical memories are attractive because they offer high storage density and large degrees of parallelism. Various types of optical memories have been proposed and demonstrated.[1-4] Among them is time-domain optical memory (TDOM), which is based on a coherent optical phenomenon known as stimulated photon echoes.[5-8] This technique has some distinct advantages over other optical approaches to data storage, such as persistent spectral hole burning[1,2] and photorefractive effects.[3] These advantages include the high write and read speeds and the ability to process stored (both spatial and temporal) information.[9-11] The latter is particularly important in a high-density storage device because it provides the means of intelligently handling the large volumes of stored information to simplify retrieval.

The storage of two-dimensional (2-D) images in TDOM has been demonstrated in both gases and rare-earth solids.[7,12,13] Further studies have found that TDOM is also capable of processing images, such as two-image convolution and correlation, because of its inherent storage–retrieval mechanism.[11] This discovery led to its recent successful application to high-speed pattern recognition.[14]

However, several issues regarding image storage and image processing, such as the fidelity of the retrieved images, their spatial resolution, and the probable causes of various image distortions, have not been addressed. These issues are crucial in evaluation of TDOM. In addition, the ability of TDOM to process 2-D images has not been fully demonstrated. For example, two-image convolution has not been studied experimentally.

The purpose of this study was (1) to carefully examine the quality of the images retrieved from a TDOM so that issues such as image fidelity and spatial resolution could be addressed and (2) to explore the full potential of TDOM for image processing. As an important part of this work, we also studied the feasibility of using fiber optics for image input and output in TDOM. Because the retrieved (or echo) images in TDOM are phase-conjugate replicas of the data images,[7,11] it is possible to input images through fibers into the memory and to restore them to their original form as they are retrieved.

2. Background

The details regarding the mechanisms by which optical information is stored in a TDOM have been covered extensively elsewhere.[5,15,16] Here, we only summarize how the image storage–retrieval processes take place in TDOM.

Stimulated photon echo is a coherent phenomenon in which coherent radiation from materials occurs as a result of interaction with laser pulses. The optical information carried by laser pulses (images or simple

digital pulses) is stored in the electronic states of the storage materials through resonant excitations. In rare-earth solids, for example, the information is stored in the electronic states of rare-earth ions such as Eu^{3+} and Pr^{3+}. The entire storage–retrieval process involves the use of a write pulse and a read pulse in addition to the data pulses to be stored.

To simplify our discussion, consider the storage of one data pulse, which occurs before the write pulse. Because of the difference in local strain experienced by each ion in the crystal, the energy spectrum associated with a given electronic transition is broadened, which is known as inhomogeneous broadening. After the interaction with the data pulse at t_1, a portion of the ions are resonantly excited by the laser pulse. Because the process is coherent, each excited ion memorizes its initial phase (determined by the laser radiation) and oscillates at its own resonant frequency. Thus the temporal information of the data pulse is converted into spectral information by the crystal.

When the write pulse arrives at t_2, it interferes with the effect of the data pulse through laser-material interactions: if the dipoles of the excited ions are in phase with the write pulse, the interference is constructive; otherwise, it is destructive. This interference, similar to the spatial interference of two coherent laser beams in holography, contains the complete information of the combined laser pulses.

If the storage material were a simple two-level system, the storage time would be determined by the lifetime of the excited state, and long-term data storage would not be possible. However, in rare-earth solids, as one example, hyperfine structures exist in the ground state, and the excited ions are likely to decay to hyperfine sublevels different from the one at which the excitation was originated. Thus the spectrally modulated population distribution generated by the data and write pulses can persist in the hyperfine states for a long time. A storage time of several hours has been demonstrated.[8]

To recall stored information from the hyperfine sublevels, we re-excite the crystal by the real pulse at t_3. This pulse induces coherent radiation (known as echoes) from the crystal at $t_e = t_3 + (t_2 - t_1)$. The temporal profile of the echo is proportional to the Fourier transform of the spectrally modulated ground-state population distribution. In the limit of small pulse areas, we can obtain this profile by performing a temporal correlation between the write and read pulses and then by convoluting the result with the data pulse.[9] Thus for pulses with symmetric temporal profiles the resulting echo envelope is also symmetric with a length greater than (or equal to) that of the longest pulse among the three inputs. Since our discussion focuses on the storage of spatial information, we consider here only the spatial part of the echo pulse. It can be shown that the spatial part of the

induced macroscopic polarization P has the form[15]

$$P \propto u_1^*(x, y)u_2(x, y)u_3(x, y)\exp[i(-\mathbf{k}_1 + \mathbf{k}_2 + \mathbf{k}_3)\mathbf{r}],$$

(1)

where u_i is the spatial modulation envelope of the ith pulse and $\mathbf{k}_i$ is the wave vector of that pulse (assuming the input-pulse electric field has the form $E_i = A_i(x, y, t)\exp[i(\mathbf{k}_i\mathbf{r} - \omega_0 t)] + \text{c.c.}$). If the write ($i = 2$) and read pulses ($i = 3$) are spatially uniform, P is proportional to $u_1^*(x, y)$. Thus the stored image is recalled. If, in addition, a counterpropagating geometry is used (i.e., $\mathbf{k}_2 = -\mathbf{k}_3$), the recalled image is a phase-conjugate replica of the data image propagating in the direction opposite that of the data pulse.

The ability to process 2-D images can be readily seen from relation (1). If the Fourier-transformed images are stored instead, P will be proportional to the product of the three transformed input images. And if, in addition, the echo image is Fourier transformed back upon retrieval, then it can be shown[11,17] that the spatial modulation envelope of the image detected is

$$E_e \propto u_3(-x, -y) \otimes u_2(-x, -y) * u_1(-x, -y),$$ (2)

where $\otimes$ and $*$ are the spatial Fourier correlation and convolution, respectively. Relation (2) states that, if u_1 is a delta function, the echo image is a convolution of u_2 with u_3. If, instead, u_2 (or u_3) is a delta function, then the echo is a correlation of u_3 (or u_2), with u_1.

Spatial Fourier transformations can be accomplished by use of converging lenses[18]; however, caution must be taken to ensure that the Fresnel approximation is satisfied. For a given system this approximation limits the maximum obtainable spatial frequency as well as the sample thickness. Under this condition the sample must be much thinner than the focal depth determined by the confocal parameter. A detailed discussion on the use of converging lenses for image processing has been presented elsewhere.[17]

The above analysis of TDOM can be easily generalized to the storage of multiple images. However, with the choice of the first pulses as a data pulse train, the retrieved images are the time-reversed replicas of the data images.[19–21]

3. Experimental Apparatus

The experimental setup is sketched in Fig. 1 along with the temporal sequence of the input and echo pulses. This is a typical setup for a three-pulse backward-echo experiment. We chose this geometry because the input laser pulses are spatially separated, permitting the spatial modulation of individual pulses for the purpose of image processing. In addition, this geometry permits the use of optical fiber for image transmission, as is discussed in Section 4. The experiments were performed on the $^3P_0$–$^3H_4$ transition in a Pr^{3+}:LaF_3 crystal (0.1 at %, 6-mm diameter, and 1-mm thick), which was mounted in a
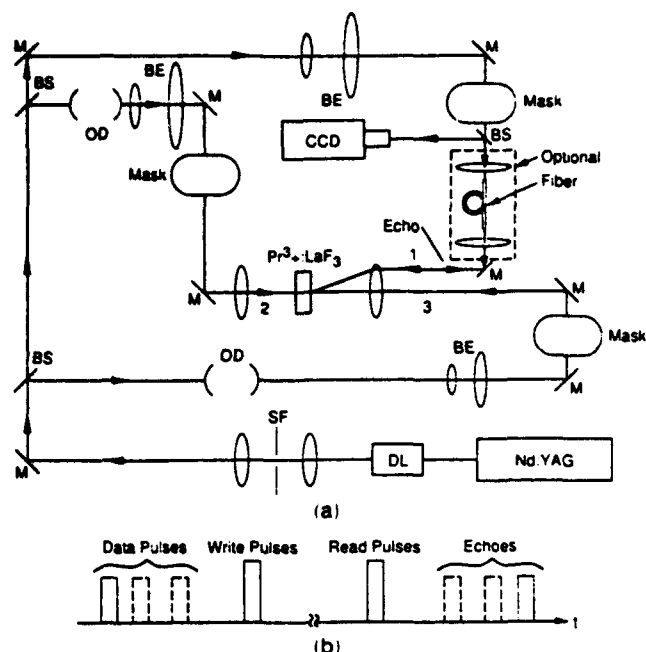
Fig. 1. (a) Schematic of the experimental apparatus for image storage and image processing in TDOM: BS's, beam splitters; BE's, beam expanders; M's, mirrors; DL, dye laser; OD's, optical delay lines; CCD, intensifier CCD camera; SF, spatial filter. The part labeled Optional is used to demonstrate phase conjugation. (b) Temporal sequence of the input and echo pulses.

flowing helium vapor cryostat at ~6 K. $Pr^{3-}:LaF_3$ was chosen because it has a short storage time (~100 ms), which permitted us to run experiments at 10 Hz.

A Nd:YAG (Quanta-Ray DCR-3) pumped, pulsed dye laser was used to resonantly excite the $Pr^{3-}:LaF_3$ crystal at 477.8 nm. The laser pulses (~5-ns long and 10-GHz linewidth) were first split into three parts by beam splitters, two of which were optically delayed by use of a White cell delay line. A spatial filter was installed before the beam splitters to improve the spatial profile of the laser pulses. The individual laser pulses were expanded and collimated with beam expanders to illuminate transmission masks, and the images generated by the masks were then focused onto the sample in a nearly coaxial configuration. The masks were placed at the front focal plane of the transform lenses, while the sample was placed at the back focal plane, as shown in Fig. 1. This arrangement ensures the exact Fourier transforms of the input images at the sample. Here, the focal length of the transform lenses was 400 mm, and the separation angle between the first and second pulses was approximately 2°. The echo emitted in the direction opposite that of the data pulses (owing to the phase-matching requirement) was detected by a gated intensified CCD camera (Stanford Computer Optics, 4 Quik-05) with the aid of a 50/50 beam splitter and digitized by a frame grabber. The transmission masks used in the present experiment were black-and-white transparencies except for the resolution chart (Newport Corporation), which was a glass substrate coated with opaque chrome.

For a simple image storage–retrieval experiment we removed the transmission masks and the beam expanders for the second and third pulses, and we collimated the laser beams at the sample to simulate delta function masks. Thus the recorded image is the phase-conjugate replica of the data image [relation (1)]. The relative delays between the first (data) and second (write) pulses and between the second and third (read) pulses were 90 and 20 ns, respectively, and the energy of the individual laser pulses was approximately 30 μJ.

4. Results and Discussion

A. Two-Dimensional Image Storage and Retrieval

To examine the fidelity and spatial resolution of the retrieved images, we consider here the storage of only one data image. Issues related to the storage of multiple images, such as cross talk, have been addressed elsewhere.[14]

The transmission mask for the data pulse here was a resolution target consisting of the standard U.S. Air Force pattern. The write and read pulses were plane waves to simulate delta function masks. Figure 2 shows both the input image to be stored and the echo image retrieved from the memory. Here the retrieved image was recorded from a single echo event by the CCD camera and digitized by the frame grabber; no signal averaging was performed. It is clear from Fig. 2 that the retrieved image is of good
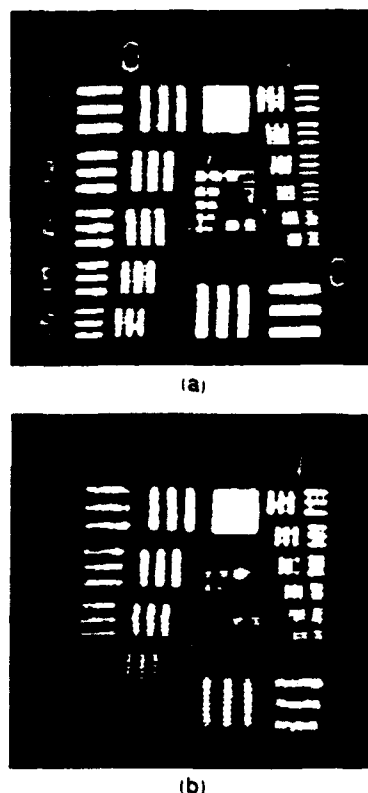

Fig. 2. Experimental results showing the fidelity and spatial resolution of the image retrieved from TDOM: (a) input data image (resolution chart), (b) echo image.

B-3

quality; no apparent distortions were detected. The closest line pairs resolved in the measurement were approximately 3.17 line pairs/mm (i.e., group 1, element 5).

Careful examination shows that the measured spatial resolution was limited primarily by the recording system (i.e., the CCD camera) and does not represent the intrinsic resolution of the memory. We believe that this limit in the spatial resolution was determined largely by the blooming effect in the microchannel-plate intensifier, which was caused by high instantaneous echo power detected by the CCD camera. Although the total echo energy in the experiment was low (~ 1 nJ) here, the instantaneous power was of the order of several watts because of the short pulses.

Since we stored here a Fourier-transformed image in a small sample area (determined here by the size of the write–read pulses to be ~ 2 mm in diameter), the high-frequency components of the input image were not entirely collected, so the retrieved image was not as sharp as the input image, as evident in Fig. 2. This effect, however, can be removed if larger write–read beams are used.

The use of the first pulse as a data pulse in this counterpropagating geometry ensures high-quality echo images because the recalled image is a phase-conjugate replica of the data image (as discussed in Section 2), and any distortion caused by optics is removed upon retrieval. We also examined the use of the second pulse as a data pulse, and the results showed measurable differences in image quality. This unique property relaxes considerably the requirements on the imaging optics of the memory and even permits the use of optical fibers for image transmission.

B. Image Storage and Retrieval Through an Optical Fiber

Image information, encoded as a spatial intensity pattern, is rapidly scrambled as it propagates in an optical fiber because of mode coupling.[22] The only method known thus far to restore an image scrambled by an optical fiber is to use a phase-conjugating mirror and to retransmit the scrambled image through an identical fiber link. This finding limits the practical use of optical fibers for image transmission.

We present here an example in which optical fibers are used for image transmission in a practical image-storage device. As discussed earlier, if the first input pulse is used as a data pulse, the time-domain optical memory is essentially a delayed phase-conjugating mirror. Therefore the scrambled echo images, after being transmitted through the same fiber that creates the distortion during data storage, are restored to their original undistorted form upon retrieval.

Figure 3 shows experimental results that demonstrate such an application to image transmission. Here the input image was first focused into a multimode fiber (400-μm diameter and 40-cm long) by use of a 400-mm focal-length lens. The output from the fiber was then imaged onto the sample (see the portion labeled Optional in Fig. 1). No other changes
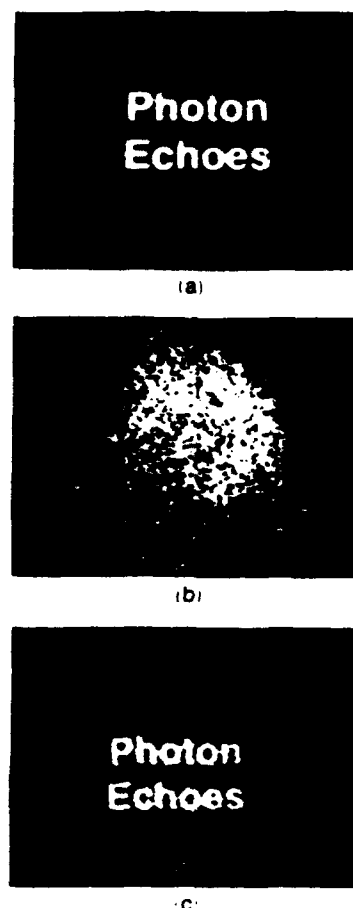

Fig. 3. Experimental demonstration of phase conjugation: (a) input data image, (b) after passage through a multimode optical fiber, (c) echo image retrieved.

to the experimental apparatus were made. As expected, the input image was completely scrambled after being transmitted through the fiber [Fig. 3(b)]. However, when the scrambled image was stored and later retrieved through the same fiber, we detected a restored image, as shown in Fig. 3(c).

These results have important implications for the development of TDOM. With optical fibers the memory can be more compact and requires no optical alignment. Furthermore, multiple fibers can be used to simultaneously store and retrieve many images to increase further the data throughput rate or to store large images that cannot be handled by lens systems. Another potential application of this fiber-based optical memory would be a multiuser central system, in which each user's data are stored through an optical fiber in one memory location in the central system. This approach would significantly reduce the cost as well as the effort of keeping the storage material at required low temperatures. However, issues such as the effect of fiber thermal fluctuation on retrieved images must be carefully studied before implementation of this technique.

C. High-Speed Image Processing

The unique storage–retrieval mechanism of TDOM permits its use for high-speed image processing, as

discussed earlier. Xu et al. have demonstrated the operation of two-image correlation by using TDOM.[11] However, because these authors used transmission masks with high degrees of symmetry, they were unable to demonstrate certain features of spatial correlation. In addition, two-image convolution available with TDOM has not been studied experimentally.

To demonstrate two-image convolution and correlation with clarity, we used transmission masks with low degrees of symmetry, such as the numerals 5 and 7. The horizontal direction (from left to right) of the masks was chosen to be the x axis, and the vertical direction (from bottom to top) was chosen to be the y axis. The z axis (here we use the right-hand coordinate system) was chosen to be along the same direction as that of the second (write) pulse. Our experimental results (summarized in Fig. 4) show that the two-image correlation operations [Figs. 4(a) and 4 b] are not symmetric with respect to the order of the inputs, but the convolution operations are [Figs. 4(c) and 4(d)]. Figure 4 further shows that, if the second pulse were used as a data pulse, the retrieved image would be inverted ($x \rightarrow -x, y \rightarrow -y$), as predicted by relation (2).

This demonstrated processing ability, along with its potentially high storage density, makes TDOM an ideal candidate for high-speed pattern recognition. A large data base can be created before processing by storage of reference images into the memory sequentially with a single write pulse. The unknown spatial information to be analyzed (or the data image is carried by the read pulse at a later time. Under this condition the echoes, generated upon the arrival of the data image, are the spatial correlations between

the data image and every reference image. Since the temporal sequence of the echo pulses is uniquely related to that of the reference pulses, the reference image that yields high spatial correlation with the data image can then be identified from the corresponding echo image. Such an application to pattern recognition has been recently demonstrated successfully in our laboratory.[14]

Further applications of TDOM include optical interconnects, in which the stored images can be directed simultaneously to many output ports by use of an appropriately encoded read pulse. Figure 4(c) demonstrates such an application, in which the stored numeral 7 was sent simultaneously to three output ports by the read pulse. The advantage of this approach to optical interconnects is its rapid reprogrammability. This output ports can be changed every time a read command is issued.

The quality of the echo images obtained here may be improved further by use of a coaxial geometry, because under this condition the phase-matching requirement is met in the entire Fourier plane. Other possible improvements include the use of large storage crystals to accommodate high spatial frequency components for sharp echo images.

5. Conclusion

We have examined the use of the time-domain optical memory for image storage and image processing. Our results suggest that the first pulse should be used as a data pulse to carry spatial information for image storage, since under this condition the retrieved image is the phase-conjugate replica of the data image. This unique feature not only ensures the recall of distortion-free images but also permits the use of optical fibers for image transmission. The latter opens the possibility of development of fiber-optics-based image-storage devices.

The inherent image-processing capability of TDOM provides unprecedented flexibility in the handling of stored information, making it an ideal candidate for high-speed pattern recognition and optical interconnections. Combining these features with the temporal processing ability demonstrated elsewhere,[9,10] TDOM shows an incomparable potential to be a high-performance high-density massively parallel optical memory with features such as content-based retrieval.

Fig. 4. Experimental results showing the use of TDOM to perform the following: (a), (b) two-image correlations; (c), (d) two-image convolutions.

References and Notes

1. G. Castro, D. Haarer, R. M. Macfarlane, and H. P. Trammsdorff, "Frequency selective optical data storage," U.S. patent 4,101,976 (18 July 1978); A. Szabo, "Frequency selective optical memory," U.S. patent 3,896,420 (22 July 1975).

2. W. E. Moerner, "Molecular electronics for frequency domain optical storage: persistent spectral hole-burning: a review," J. Mol. Electron. 1, 55–71 (1985).
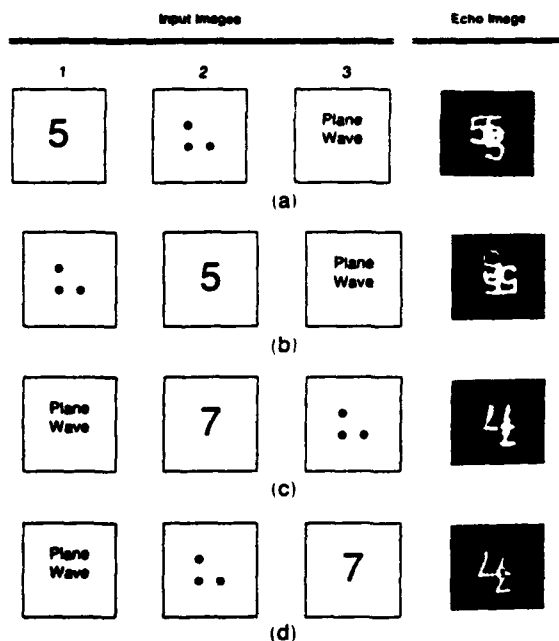
B-5

3. See, for example, P. Gunter and J. P. Huignard, eds., *Photore-fractive Materials and Applications* (Springer-Verlag, New York, 1988), Vols. 1 and 2.

4. S. Hunter, F. Kiamilev, S. Esener, D. A. Parthenopoulos, and P. M. Rentzepis, "Potentials of two-photon-based three-dimensional memories for high performance computing," Appl. Opt. **29**, 2058–2066 (1990).

5. I. D. Abella, N. A. Kurnt, and S. R. Hartmann, "Photon echoes," Phy. Rev. **141**, 391–406 (1966).

6. T. W. Mossberg, "Time domain data storage," U.S. patent 4,459,682 (10 July 1984); "Time-domain frequency-selective optical data storage," Opt. Lett. **7**, 77–79 (1982).

7. Y. S. Bai, W. R. Babbitt, and T. W. Mossberg, "Coherent transient optical pulse-shape storage/recall using frequency-swept excitation pulses," Opt. Lett. **11**, 724–726 (1986).

8. M. K. Kim and R. Kachru, "Multiple-bit long-term data storage by backward-stimulated echo in Eu^{3+}:YAlO$_3$," Opt. Lett. **14**, 423–425 (1989); "Long-term image storage and phase conjugation by a backward-stimulated echo in Pr^{3+}:LaF$_3$," J. Opt. Soc. Am. B **4**, 305–308 (1987).

9. Y. S. Bai, W. R. Babbitt, and T. W. Mossberg, "Real-time optical waveform convolver/cross correlator," Appl. Phys. Lett. **45**, 714–716 (1984).

10. X. A. Shen, Y. S. Bai, and R. Kachru, "Reprogrammable optical matched filter for biphase-coded pulse compression," Opt. Lett. **17**, 1079–1081 (1992).

11. E. Y. Xu, S. Kroll, D. L. Heustis, and R. Kachru, "Nanosecond image processing using stimulated photon echoes," Opt. Lett. **15**, 562–564 (1990).

12. N. W. Carlson, W. R. Babbitt, and T. W. Mossberg, "Storage and phase conjugation of light pulses using stimulated photon echoes," Opt. Lett. **8**, 623–625 (1983).

13. M. K. Kim and R. Kachru, "Storage and phase conjugation of multiple images using backward-stimulated echoes in Pr^{3+}:LaF$_3$," Opt. Lett. **12**, 593–595 (1987).

14. X. A. Shen and R. Kachru, "High-speed pattern recognition by using stimulated echoes," Opt. Lett. **17**, 520–522 (1992).

15. T. W. Mossberg, R. Kachru, S. R. Hartmann, and A. M. Flusberg, "Echoes in gaseous media: a generalized theory of rephasing phenomena," Phys. Rev. A **20**, 1976–1996 (1979).

16. M. Fujita, H. Nakatsuka, H. Nakanishi, and M. Matsuoka, "Backward echo in two-level systems," Phys. Rev. Lett. **42**, 974–977 (1979).

17. D. M. Pepper, J. AuYeung, D. Fekete, and A. Yariv, "Spatial convolution and correlation of optical fields via degenerate four-wave mixing," Opt. Lett. **3**, 7–9 (1978).

18. J. W. Goodman, *Introduction to Fourier Optics* (McGraw-Hill, New York, 1968), pp. 77–100.

19. N. S. Shiren, "Generation of time-reversed optical wave fronts by backward-wave photon echoes," Appl. Phys. Lett. **33**, 299–300 (1978).

20. N. W. Carlson, Y. S. Bai, W. R. Babbitt, and T. W. Mossberg, "Temporally programmed free-induction decay," Phys. Rev. A **30**, 1572–1574 (1984).

21. M. Mitsunaga and R. G. Brewer, "Generalized perturbation theory of coherent optical emission," Phys. Rev. A **32**, 1605–1613 (1985).

22. A. Yariv, "Three-dimensional pictorial transmission in optical fibers," Appl. Phys. Lett. **28**, 88–89 (1976).

Appendix C

HIGH-SPEED PATTERN RECOGNITION BY USING STIMULATED ECHOES

High-speed pattern recognition by using stimulated echoes

X. A. Shen and R. Kachru

Molecular Physics Laboratory, SRI International, Menlo Park, California 94025

We present experimental results demonstrating the use of stimulated echoes for high-speed pattern recognition. One data image and two reference images (spatially encoded laser pulses) were stored and processed in a Pr^{3+}:LaF_3 crystal by focusing the pulses sequentially into the storage material. The processed information was later retrieved by a read pulse, generating two temporally separated echo images that are the spatial correlations between the data and reference images. Identification of the data image was accomplished by finding the echo image that showed the highest spatial correlation with the data image. The present processing speed is 30 ns per correlation operation.

The use of stimulated echoes to store a two-dimensional image was first demonstrated in gas by Carlson *et al.*[1] and subsequently in rare-earth solids by Kim and Kachru.[2] The work was later extended to the storage of two images, and the results show no measurable cross talk between the inputs.[3] Recently Xu *et al.*[4] demonstrated the use of backward stimulated echoes for high-speed image processing and showed that two-image correlation and convolution can be operated on a nanosecond time scale. This dual ability to store and process images makes the stimulated-echo technique a potential candidate for high-speed pattern recognition.

Existing methods for pattern recognition, such as digital computer processing, Van der Lugt holography,[5] neural networks,[6] and four-wave mixing in photorefractive materials,[7-9] suffer from two major disadvantages: slow processing speed and very limited memory capacity. To make pattern recognition practical, one would have to develop a high-speed processor that compares the unknown test image with a potentially large number of reference images. Thus far no such device is available. In this Letter we demonstrate the use of stimulated echoes for nanosecond pattern recognition. We show that this technique has the potential to meet the needs discussed above, i.e., high storage density and high processing speed.

The approach to pattern recognition used here is based on the concept of performing high-speed correlation between a data image (i.e., an unknown image to be analyzed) and every reference image stored in the data base. Three spatially encoded laser pulses, one representing a data image and the others representing reference images, are focused sequentially into a rare-earth solid (0.1 at.% Pr^{3+}:LaF_3) at 477.8 nm, a laser wavelength resonant with the $^3P_0$–$^3H_4$ transition of the crystal. The images are thus stored and processed in the Pr^{3+}:LaF_3 crystal, and the processed information is later retrieved by another laser pulse (read pulse), generating two echo images that are separated in time. Each of the echo images is the spatial correlation between the data image and one of the reference images. Since

the temporal sequence of the echo pulses is related uniquely to that of the reference pulses, the reference image that yields high spatial correlation with the data image can then be identified from the corresponding echo image.

The storage of optical information in stimulated photon echoes is accomplished through spectral interference created in the storage material on interaction with two (or more) temporally separated laser pulses. This interference, similar to the spatial interference of two coherent light beams in holography, contains the complete information about the combined laser pulses.[10] Consider a simple three-pulse echo experiment in which the center laser frequency is ω_0. The three pulses interact sequentially with a sample consisting of an assembly of ions whose center absorption frequency is equal to the laser frequency. On interaction of the first pulse with these ions, at time t_1, a fraction of the ions are excited from their ground state to the excited state by absorbing laser photons. Owing to the coherent nature of the laser pulse, the transition dipoles of all the excited ions, immediately after the interaction, will have an identical phase determined by the laser pulse. However, because of the presence of inhomogeneous broadening, each excited ion oscillates at its own frequency ω, which may differ from the laser frequency. When the second laser pulse arrives, at t_2, it interferes with the effect of the first pulse differently for each excited ion because of the different amounts of phase accumulated by the dipoles of the ions. If the dipoles are in phase with the second pulse at t_2, the interference is constructive; otherwise it is destructive. Thus the population of electrons in the ground and excited states is spectrally modulated, and this modulation contains the complete information about the combined laser pulses. Owing to the presence of the ground-state hyperfine structures in rare-earth ions, the spectrally modulated population distribution can persist for a long time in the hyperfine states. A storage time of several hours was recently demonstrated in Eu:YAlO3.[11]

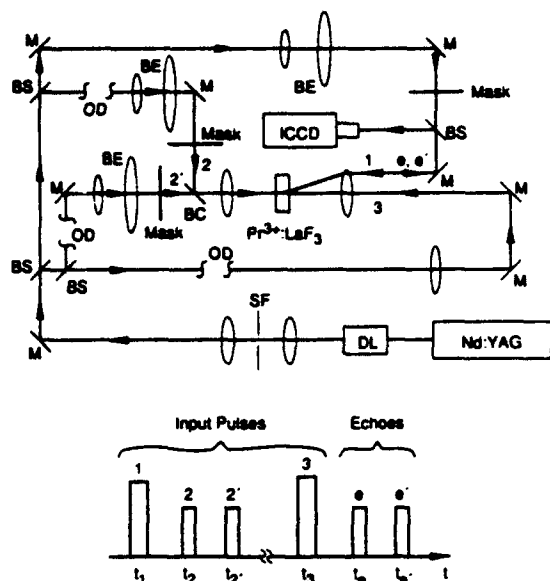The effect of the read pulse on the storage mate-

Fig. 1. Schematic of the experimental setup for high-speed pattern recognition. The temporal sequence of the input and echo pulses is also shown. DL, dye laser; SF, spatial filter; M's mirrors; BS's, beam splitters; OD's, optical delays; BE's, beam expanders; BC, beam combiner; ICCD, intensified CCD camera.

rial at t_3 is to induce coherent radiation (an echo) whose temporal profile is proportional to the Fourier transform of the frequency-labeled ground-state population distribution. Since this distribution is spectrally modulated, the induced macroscopic polarization P at a time (echo time) $t_e = t_3 + (t_2 - t_1)$, in the limit of small pulse area,[10] can be shown to have the form

$$P \propto u_1^* u_2 u_3 \exp[i(-\mathbf{k}_1 + \mathbf{k}_2 + \mathbf{k}_3) \cdot \mathbf{r}], \qquad (1)$$

where u_i is the amplitude modulation of the electric field of the ith laser pulse and $\mathbf{k}_i$ is the wave vector of the pulse. The information of the input laser pulses is thus retrieved.

The ability to process two-dimensional images can be readily seen from relation (1). If instead the Fourier-transformed images are stored, P will be proportional to the product of the three transformed images. If, in addition, the echo image is Fourier transformed again on retrieval, then the resulting amplitude of the echo electric field E_e is related to the three input images through the following relation[4,7]:

$$E_e(x, y) \propto u_1(-x, -y) \otimes u_2(-x, -y) * u_3(-x, -y), \qquad (2)$$

where $\otimes$ and $*$ represent the spatial Fourier correlation and convolution, respectively. Relation (2) states that if u_1 is a delta function, the echo image is a convolution of u_2 and u_3. If instead u_2 (or u_3) is a delta function, the echo image is a correlation of u_1 and u_3 (or u_2).

Spatial Fourier transformations can be accomplished by using converging lenses. It is known that if an object mask (used to spatially modulate a laser pulse) is placed at the outer focal plane of a trans-form lens, the resulting image at the inner focal plane is an exact Fourier transform of the object mask.[12] Thus input images can be Fourier transformed by use of this lens geometry before storage. When the stored information is later retrieved, it is Fourier transformed back by the lens, the result being an echo image whose electric field amplitude is given by relation (2).

The above analysis can be generalized to cases in which one of the pulses is replaced by a pulse train. In the present experiment the second pulse is replaced by two small pulses to represent reference images. It can be shown that this arrangement produces two echo images, one at $t_e = t_3 + (t_2 - t_1)$ and the other at $t_{e'} = t_3 + (t_{2'} - t_1)$, each of which has the form given by relation (2).

Figure 1 shows the experimental arrangement along with the temporal sequence of the laser and echo pulses. A Nd:YAG-laser-pumped, pulsed dye laser with a 10-GHz linewidth and a 5-ns pulse width was used to excite resonantly the Pr^{3+}:LaF$_3$ crystal at 477.8 nm. The laser pulse, after passage through a spatial filter, was divided into four parts by using beam splitters, and three of these parts (pulses 2, 2', and 3) were optically delayed by using a White cell delay line. Pulses 1, 2, and 2' were then expanded to a diameter of approximately 25 mm by telescopes to illuminate the object masks (black-and-white transparencies). The energies of the input pulses ranged from 30 to 50 μJ. Two achromatic doublets of 40-mm focal length were used coaxially to focus the images into the crystal.

Since counterpropagating geometry was used here, pulses 2 and 2' propagated collinearly along the optical axis in the direction opposite to the read pulse (pulse 3). Pulse 1 was focused by one of the doublets at a 30-mrad angle to the direction of the read pulse. To simulate a delta-function mask for pulse 3 (equivalent to a plane wave at the sample), we placed a third lens outside the two-lens system to collimate the beam at the sample. Pulses 1, 2, and 2' were sequentially focused into the sample, and the delays of pulses 2, 2', and 3 relative to the first pulse were 85, 115, and 130 ns, respectively. The Pr^{3+}:LaF$_3$ sample (6-mm diameter, 1-mm thickness) was mounted in a liquid-helium cryostat, and the temperatures used in the experiment varied between 6 and 8 K. We chose Pr^{3+}:LaF$_3$ for the demonstration because it has a short storage time (~100 ms) and thus permitted us to run experiments at 10 Hz for convenience.

The echo pulses that propagated in the direction opposite to the first pulse were Fourier transformed by the doublet (see Fig. 1), and the resulting images at the outer focal plane were recorded by a gated intensified CCD camera (Stanford Computer Optics, 4 Quik-05) and digitized by a frame grabber. We used a 50-ns pulse to gate the intensified CCD to permit detection of individual echo images.

To ensure that the operations of spatial correlation were correct, we first tested the experimental apparatus with the following masks: a numeral 7 for pulse 1, two vertically (or horizontally) separated dots for pulse 2 (or pulse 2'), and a plane wave for the
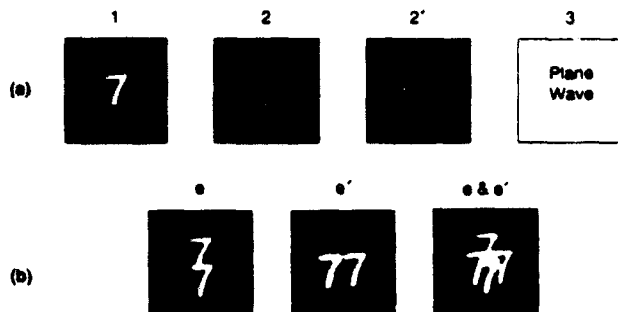
Fig. 2.   (a), (b) Photographs show`ng two successive operations of a two-image correlation. The two echo images (e and e') were separated by 30 ns and recorded individually by the gated intensified CCD camera. The last photograph in (b) shows the simultaneous recording of the two echo images.
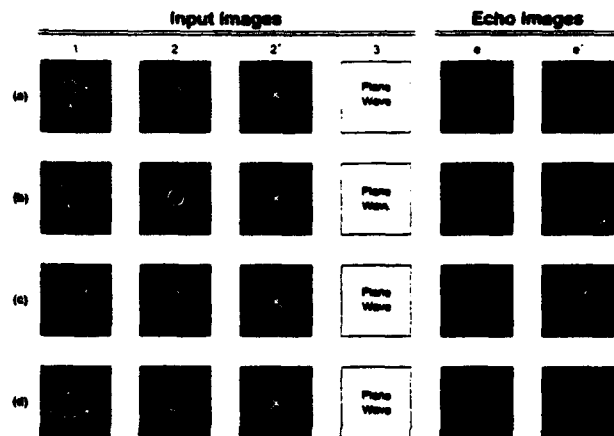

Fig. 3.   Photographs demonstrating nanosecond pattern recognition. Pulse 1 is the data image to be analyzed, and pulses 2 and 2' are the reference images. (a) Correlations of the reference images with a data image consisting of two O's and two X's. (b) After the right side of the data image in (a) is blocked. (c) After the left side of the data image in (a) is blocked. (d) After the data image in (a) is rotated by 90°.

read pulse (pulse 3). The experimental results are shown in Fig. 2. The first recorded echo image is two 7's separated vertically, representing the correlation of pulses 1 and 2. The second echo image is also two 7's, but the two are separated horizontally, representing the correlation of pulses 1 and 2'. The last picture shows the simultaneous recording of the two echo images. Figure 2 clearly demonstrates two successive operations of spatial correlation. No cross talk between input images was detected.

To demonstrate pattern recognition using stimulated echoes, we chose a mask that consists of two O's and two X's for the data pulse, as shown in Fig. 3(a). The masks for the reference images were an O for pulse 2 and an X for pulse 2'. The first echo image (e) shows two bright points located in the upper left and lower right areas, indicating that these two parts of the data image are highly correlated with the pattern O. Indeed, the data image, as shown in the figure, was encoded with a pattern O in each of the areas. The second echo image (e') also shows two bright points, but the two points are

rotated by 90° compared with the first echo, which indicates the high spatial correlation between the reference pattern X and the corresponding parts of the data image. When the right (or left) side of the data image was blocked, as shown in Fig. 3(b) [or Fig. 3(c)], we detected, as expected, only one bright point for each echo image. When the data image was rotated by 90°, the corresponding echo images were also rotated [Fig. 3(d)]. The results here were recorded from single echo images by using the gated CCD; no signal averaging was involved.

The present technique can, in principle, be applied to a large number of reference images. Kröll et al.[13] have successfully demonstrated the storage of 48 optical data pulses in $Pr^{3+}:YAlO_3$. A density of 10^5 images in a 1-cm^2 sample is feasible by using the present approach to data storage.

In the present study of pattern recognition, the image storage and image processing were carried out simultaneously in the storage medium. As stated earlier, the stimulated-echo technique is capable of performing these two operations separately. By replacing the first pulse with a pulse train to represent reference images, one can store these images into the processor with a single write pulse.[11] The operations of two-image correlation can be carried out at a later time, by using a read pulse that carries unknown spatial information to be analyzed. This delay can be several hours or longer.[11]

In conclusion, we have successfully demonstrated high-speed pattern recognition using the stimulated-echo technique. The achieved processing speed was 30 ns per correlation operation, and the retrieved images were of good quality. This work represents what is to our knowledge the first demonstration of pattern recognition using stimulated echoes.

References

1. N. W. Carlson, W. R. Babbitt, and T. W. Mossberg, Opt. Lett. 8, 623 (1983).
2. M. K. Kim and R. Kachru, J. Opt. Soc. Am. B 4, 305 (1987).
3. M. K. Kim and R. Kachru, Opt. Lett. 12, 593 (1987).
4. E. Y. Xu, S. Kröll, D. L. Huestis, R. Kachru, and M. K. Kim, Opt. Lett. 15, 562 (1990).
5. A. B. Van der Lugt, IEEE Trans. Inf. Theory IT-10, 2 (1964).
6. E. G. Paek and D. Psaltis, Opt. Eng. 26, 428 (1987).
7. D. M. Pepper, J. AuYeung, D. Fekete, and A. Yariv, Opt. Lett. 3, 7 (1978).
8. J. O. White and A. Yariv, Appl. Phys. Lett. 1, 37 (1980).
9. S. G. Odulov and M. S. Soskin, Sov. Phys. Dokl. 25, 5 (1980).
10. T. W. Mossberg, R. Kachru, S. R. Hartman, and A. M. Flusberg, Phys. Rev. A 20, 1976 (1979).
11. M. K. Kim and R. Kachru, Opt. Lett. 14, 423 (1989).
12. J. W. Goodman, *Introduction to Fourier Optics* (McGraw-Hill, New York, 1968).
13. S. Kröll, L. E. Jusinski, and R. Kachru, Opt. Lett. 16, 517 (1991).

Appendix D

TIME-DOMAIN HOLOGRAPHIC IMAGE STORAGE

TIME-DOMAIN HOLOGRAPHIC IMAGE STORAGE

X. A. Shen, E. Chiang* and R. Kachru
Molecular Physics Laboratory
SRI International
Menlo Park, CA 94025

ABSTRACT

We describe a practical approach to image storage in a coherent time-domain optical memory, which can be readily implemented with existing technologies. In this approach, two-dimensional images are stored holographically in narrow (≤ 1 MHz) frequency channels of a time-domain storage material, with one image per channel. Advantages of this approach include fast single-frame recording time, variable playback speeds, random frame access, and the ability to perform in-memory image processing. Experimental results demonstrating high-resolution, high-fidelity, single-channel image storage in Pr^{3+}:$YAlO_3$ with the use of a single-frequency ring laser are presented.

*Permanent address: Department of Physics, Massachusetts Institute of Technology, Cambridge, MA 02139

Image storage in coherent time-domain optical memory (CTDOM) has been demonstrated successfully by using high-power pulsed lasers.[1-2] Like photochemical hole burning[3] and photorefractives,[4] this time-domain approach to image storage has the potential of offering ultrahigh storage density and fast data access time. Unlike other optical memories, CTDOM is capable of providing ultrahigh image transfer rates and offers features such as in-memory image processing.[5] However, difficulties arise in using the conventional time-domain approach to image storage, namely multiple images per frequency channel. For example, existing image composers such as an electronically-addressed spatial light modulators (SLM) do not have switching times fast enough to accommodate the required recording speeds ($\geq$ MHz). High-power pulsed lasers are needed to make retrieved images detectable by electronic cameras. In addition, features such as random frame (or page) access and variable playback speed are not available with the conventional approach.

Here we propose a new approach to time-domain image storage. This approach not only retains those features that are unique to CTDOM, but also permits random frame access and variable playback speed. Most importantly, it can be readily implemented with the use of existing low-power cw lasers, a key requirement for a practical storage device.

In the proposed approach, two-dimensional input images are stored in narrow ($\Delta v \leq 1$ MHz) frequency channels within an inhomogeneously broadened absorption line of a rare earth solid by using a low-power cw laser, with one frame per frequency channel (Fig. 1). Each image is stored by first tuning the laser wavelength to the desired channel and illuminating the sample with two temporally separated pulses known as the reference (E_{r_1}) and the object (E_0) pulses. E_{r_1}, a spatially uniform laser pulse carrying no information, proceeds E_0 which carries the spatial information (e.g., an image) to be stored. The latter can be generated by transmitting a spatially uniform laser pulse through an SLM. The image thus recorded is a time-domain hologram

resulting from the interference of the temporally delayed pulses via interaction with dipoles in the storage material.[6,7]

The above recording procedure is repeated for subsequent input images at different channels and it can be initiated, for example, at the low frequency side of the inhomogeneous line and completed at the opposite side by incrementally increasing the laser wavelength at the corresponding input rate. For an inhomogeneous bandwidth of 6 GHz (typical of a rare earth solid) and $\Delta v = 1$ MHz, a total of 6000 images can be stored at one spatial location.

The image stored in a particular channel is recalled by tuning the laser wavelength to the channel location and exciting the sample with another reference pulse (or the read pulse, E_{r_2}), whose spatial profile is identical to that of E_{r_1}. The read pulse induces an echo which contains spatial information identical to E_o.[1,2]

The time required to record a single frame, τ_s, is determined by the temporal widths of E_{r_1} and E_o as well as their separation which can be reduced to zero with no effect on the stored information. The channel switching time can be much shorter than τ_s for the small frequency increment proposed here (i.e., ≤ 1 MHz). Thus, the upper limit of the recording speed is determined mainly by the reciprocal of τ_s, and the latter can be estimated from the efficiency of a stimulated echo.

It is important to realize that the temporal profile of an echo does not have to be identical to its input in the proposed one-frame-per-channel approach. Thus, the requirements on E_{r_1} and E_{r_2} can be relaxed considerably to permit the use of long reference pulses for efficient echo conversions with a low-power laser.

The efficiency of three-pulse echoes is found to be proportional to $\sin^2\theta_1 \sin^2\theta_2$ (here θ_i is the ith reference pulse area), with a maximum around 0.5% (i.e., when $\theta_1=\theta_2=\pi/2$).[6,7] The efficiency is defined as the ratio of the echo intensity to the object beam intensity. For convenience, we assume that the laser used for image storage is a 500 mW single-frequency cw laser

(commercially available) and that the images are reduced to approximately 1 mm × 1 mm before being stored in a CTDOM. Furthermore, the electronic transition used for image storage has a transition wavelength of 610 nm and an oscillator strength of $\sim 2 \times 10^{-8}$. Under this condition, the pulse area for a 1-μs long square pulse is approximately equal to 1, giving rise to an echo efficiency of ~ 0.25 %. If E_0 is shorter than the reference pulses, the echo length is comparable to the length of the reference pulses.[7,8] To a good approximation, we can use the latter to estimate the tot number of photons in an echo to be $\sim 4 \times 10^9$ (assuming the object pulse power is also 500 mW). For a CCD camera consisting of 1000 × 1000 pixels, this gives an average intensity of $\sim 4,000$ photons per pixel, a signal level strong enough for faithful retrieval.

The above estimate suggests that a cw laser of several hundreds of milliwatts is sufficient to store images in a CTDOM at MHz rates. This feature of fast recording speed at a modest laser power, to our knowledge, is not available with other optical techniques for image storage, including accumulated photon echoes.[9]

Unlike conventional time-domain storage,[7] the one-frame-per-channel approach permits the playback speed to differ from the recording speed. The maximum playback speed is limited only by the length of E_{r_2} and, thus, can exceed the maximum recording speed, provided that the scattered light from read pulses in adjacent frequency channels does not interfere with the echo signal. Random frame access is now possible without further modification. Another advantage is that materials with short dephasing times ($\gtrsim \tau_s$) can be used here because of the short τ_s.

To demonstrate the feasibility of using low-power lasers for image storage in the proposed scheme, we performed two-dimensional image storage in a Pr^{3+}:YAlO$_3$ crystal (~ 0.1 at. %). Figure 2 shows the schematic of the experimental apparatus. The $^3H_4$-$^1D_2$ transition of Pr^{3+}:YAlO$_3$ (a wavelength of 610.5 nm) was used and the sample (2.5-mm thick × 7-mm diameter) was mounted in a He-vapor cryostat at ~ 4 K. The reference and object pulses were generated by modulating a cw ring laser (Coherent 699, with a linewidth of ~ 1 MHz) with two acousto-optic modulators. The object pulse was expanded to approximately 2 cm in diameter to

illuminate a mask for spatial encoding. The reference pulses were also expanded and collimated by a telescope, but only to 4 mm. The arrangement of E_0 and E_{r_1} (E_{r_2}) here was chosen to be similar to those used in standard holographic data storage, i.e., E_0 and E_{r_1} (E_{r_2}) propagate along different directions and intersect at the sample as shown in Fig. 2 (here the intersecting angle was ~8°). Instead of imaging the input on the sample to the size required for efficient echo generation, we used a single lens and placed it behind the mask to focus the image down to approximately 1 mm × 1 mm. An identical lens was used behind the sample to reconstruct the focused image back to its original form which was then detected by a gated intensified CCD camera (a 6 mm × 4.5 mm CCD chip with 610 × 488 pixels). The separation between the mask and focusing lens was chosen to be equal to the focal length. The image thus stored was only an approximate Fourier image (because the sample was not exactly in the focal plane) and, as a result, its DC terms were spread over a much larger area in comparison to an exact Fourier image to prevent image-dependent saturation at the center.

Figure 3 shows an input (a standard U.S. Air Force resolution chart) and its echo image. The image was stored by a 5-μs long reference pulse and later recalled by a read pulse of the same length. For experimental convenience, we chose the separation between E_{r_1} and E_0 (or E_{r_2}) to be ~15 μs (or 55 μs) and the length of E_0 was 2.5 μs. The power of the three inputs was ~150 mW. Careful inspection shows that the closest line pairs resolved were >4.0 line pairs/mm (group 2 element 1). The echo image was obtained from a single storage/retrieval event with no signal averaging.

Using lenses for image storage has several advantages. The size of E_0 at the sample can be continuously adjusted to achieve optimum intensity. The recalled images are less affected by small defects in the storage materials because any variation of material quality in the Fourier plane is distributed over the entire image upon inverse transformation. Furthermore, it provides the ability to perform image processing.[4,5] For example, by encoding E_{r_2} with desired spatial information and focusing it onto the sample, the recalled image (after inverse transformation) is a convolution

of E_{r_2} with the stored image. Thus, two-image convolutions can be performed in the memory in any desired order at speeds up to MHz.

We further examined the response of echoes to grayscale inputs by using a mask (4 mm × 11 mm) consisting of six different transmission levels (Fig. 4a), and the recorded echo is shown in Fig. 4b. To quantitatively evaluate the image quality, we plotted (Figure 4c) the intensity averaged over rows (excluding the rows where numeric labels for different brightness bands were located) as a function of the column number for both the object and echo images, and found that the brightness ratios taken between adjacent transmission levels of the echo match those of the object image to within 13%. The observed low intensity in the first 40 columns in Fig. 4c arises from the presence of opaque letters printed along the side of the input, and the slow change of intensity from one brightness level to the next is caused by slight misalignment of the input image with respect to the CCD camera.

The quality of the recorded images here (both the input and the echoes) was found to be limited by the non-uniform response of the gated image intensifier in the CCD camera. Images (e.g., input images) with improved quality can be obtained by using a conventional CCD camera having no microchannel-plate intensifier. This finding suggests that the intrinsic quality of the echo images may well be higher than what was observed here. Another factor affecting the image quality is the Gaussian nature of laser spatial profiles. Spatially uniform laser beams are necessary for high-quality image storage.

In conclusion, we proposed a practical approach to image storage in CTDOM, which features random frame access, variable high recording and playback speeds, and in-memory image processing. We further performed a feasibility study of the approach by storing images into ~1-MHz wide frequency channels in $Pr^{3+}:YAlO_3$ using a low-power cw laser, and the recalled images were found to be of high fidelity.

REFERENCES

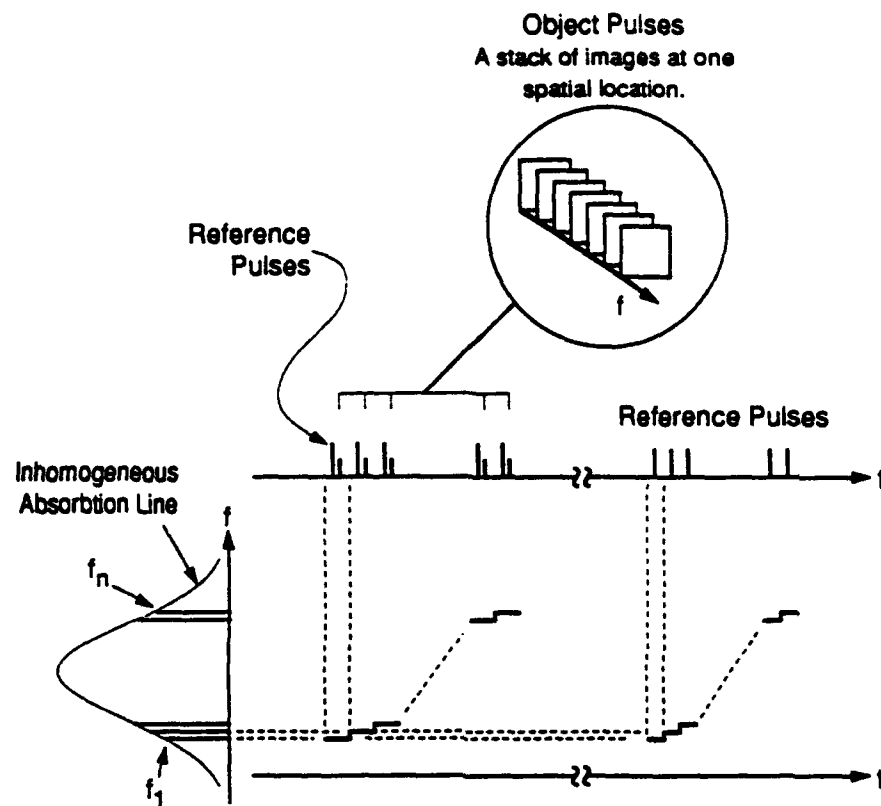1. N. W. Carlson, W. R. Babbitt, and T. W. Mossberg, Opt. Lett. **8**, 623 (1983).

2. M. K. Kim and R. Kachru, J. Opt. Soc. Am. B **4**, 305 (1987); M. K. Kim and R. Kachru, Opt. Lett. **12**, 593 (1987).

3. B. Kohler, S. Bernet, A. Renn, and U. P. Wild, in *Technical Digest on Persistent Spectral Hole-Burning: Science and Applications*, 1991 (Opt. Soc. Am., Washington, DC, 1991) Vol 16, pp 46-49.

4. F. H. Mok, M. C. Tackitt, and H. M. Stoll, Opt. Lett. **16**, 605 (1991); F. H. Mok, Opt. Lett. **18**, 915 (1993).

5. E.Y. Xu, S. Kröll, D.L. Huestis, R. Kachru, and M.K. Kim, Opt. Lett. **15**, 562 (1990); X. A. Shen and R. Kachru, Opt. Lett. **17**, 520 (1992).

6. I. D. Abella, N. A. Kurnit, and S. R. Hartmann, Phys. Rev. **141**, 391 (1966).

7. T. W. Mossberg, R. Kachru, S. R. Hartmann, and A. M. Flusberg, Phys. Rev. A **20**, 1976 (1979); T. W. Mossberg, Opt. Lett. **7**, 77 (1982).

8. Y. S. Bai, W. R. Babbitt, N.W. Carlson, and T. W. Mossberg, Appl. Phys. Lett. **45**, 714 (1984).

9. P. Saari, R. Kaarli, and A. Rebane, J. Opt. Soc. Am. B **3**, 527 (1986).

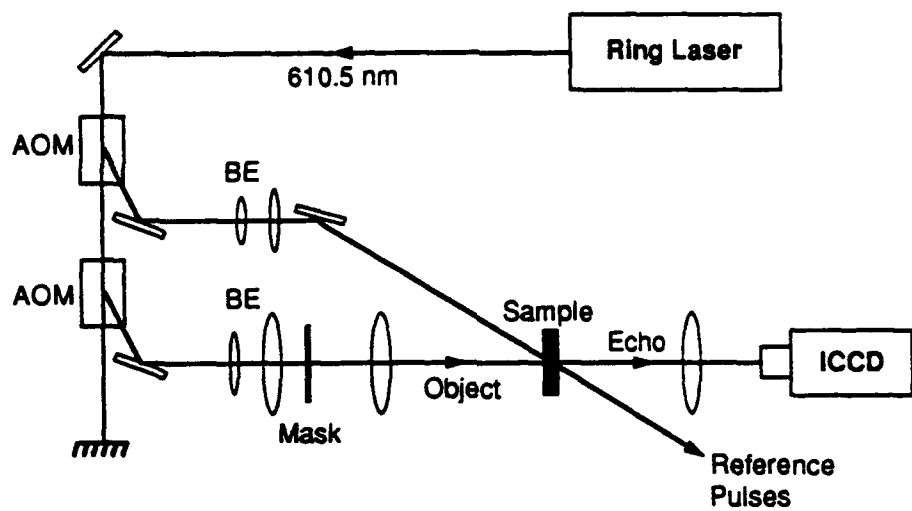# FIGURE CAPTIONS

Fig. 1   Schematic of the one-frame-per-channel approach to image storage in CTDOM.

Fig. 2   Experimental setup for time-domain holographic image storage. AOM, acousto-optic modulator, ICCD, intensified CCD camera; BE, beam expander.

Fig. 3   Experimental results demonstrating holographic image storage in CTDOM. (a) Input image (resolution chart), (b) echo image.

Fig. 4   Experimental results demonstrating the storage of grayscale inputs. (a) Input image consisting of six different transmission levels. (b) Recalled image. (c) Average intensities of the input and echo as a function of the column number.
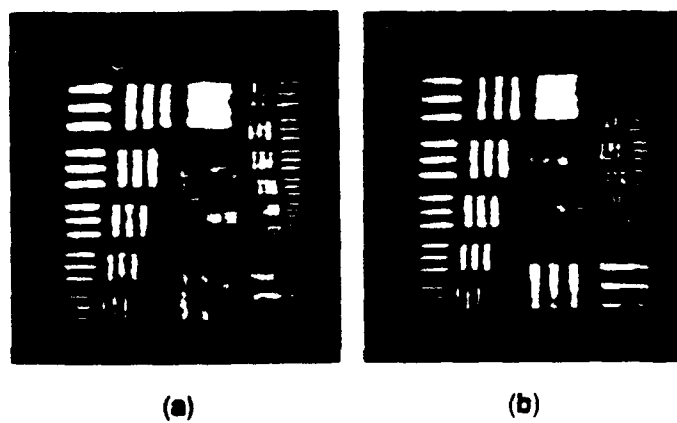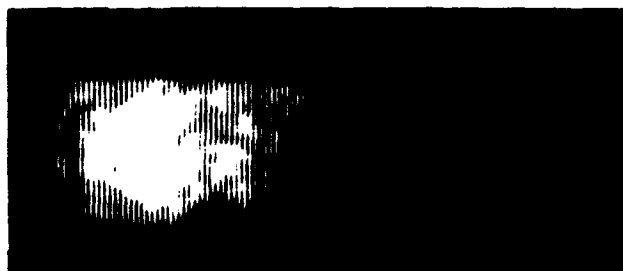
Figure 1

CM-1563-48

D-10

Ring Laser

610.5 nm

AOM

BE

AOM

BE

Mask

Object

Sample

Echo

ICCD

Reference
Pulses

CM-1563-47

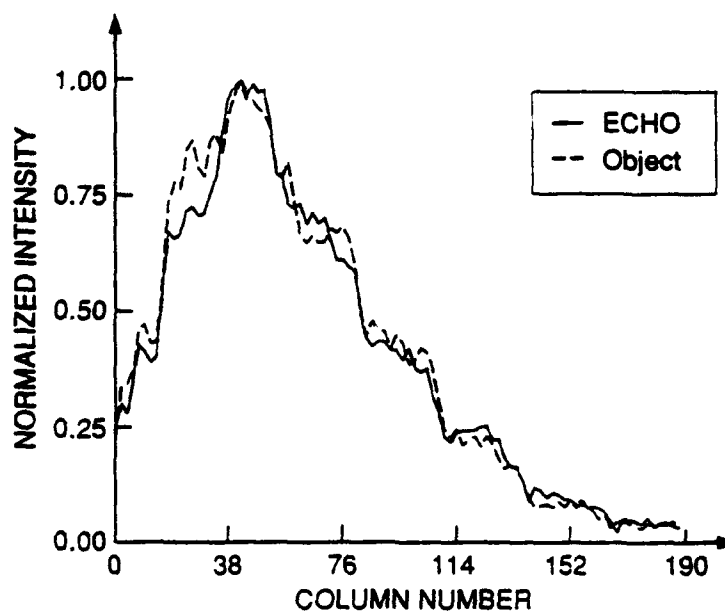Figure 2

(a)   (b)

CP-1563-45

Figure 3

(a)

(b)

(c)

CP-1563-46A

Figure 4

D-13